การตรวจแบบกึ่งหาปริมาณ RAGE cDNA ด้วยวิธี ELECTROCHEMICAL BIOSENSOR โดยใช้ HOECHST 33258

นางสาว ภาริณี กิตติมงคลสุข

วิทยานิพนธ์นี้เป็นส่วนหนึ่งของการศึกษาตามหลักสูตรปริญญาวิทยาศาสตรมหาบัณฑิต
สาขาวิชาชีวเคมีคลินิกและอณูทางการแพทย์ ภาควิชาเคมีคลินิก
คณะสหเวชศาสตร์ จุฬาลงกรณ์มหาวิทยาลัย
ปีการศึกษา 2553

SEMI-QUANTITATIVE DETECTION OF RAGE cDNA BY ELECTROCHEMICAL BIOSENSOR USING HOECHST 33258

Miss Parinee Kittimongkolsuk

A Thesis Submitted in Partial Fulfillment of the Requirements
for the Degree of Master of Science Program in Clinical Biochemistry and Molecular medicine

Department of Clinical Chemistry
Faculty of Allied Health Sciences
Chulalongkorn University

Academic Year 2010

Thesis Title	SEMI-QUANTITATIVE DETECTION OF RAGE cDNA BY ELECTROCHEMICAL BIOSENSOR USING HOECHST 33258.
By	MISS PARINEE KITTIMONGKOLSUK
Field of Study	CLINICAL BIOCHEMISTRY AND MOLECULAR MEDICINE
Thesis Advisor	ASSOCIATE PROFESSOR RACHANA SANTIYANONT, Ph.D.
Thesis Co-advisor	ASSISTANT PROFESSOR TEWIN TENCOMNAO, Ph.D.

Accepted by the Faculty of Allied Health Sciences, Chulalongkorn University in Partial Fulfillment of the Requirements for the Master's Degree

Vanida Nopponpunth ..... Dean of the Faculty of Allied Health Sciences

(Assistant Professor Vanida Nopponpunth, Ph.D.)

THESIS COMMITTEE

Wanida Laiwattanapaisal ..... Chairman

(Assistant Professor Wanida Laiwattanapaisal, Ph.D.)

R. Santiyanont ..... Thesis Advisor

(Associate Professor Rachana Santiyanont, Ph.D.)

..... Thesis Co-advisor

(Assistant Professor Tewin Tencomnao, Ph.D.)

..... Examiner

(Anchalee Chiabchalard, Ph.D.)

..... External Examiner

(Supaluk Popruk, Ph.D.)

ภาริณี กิตติมงคลสุข: การตรวจแบบกึ่งหาปริมาณ RAGE cDNA ด้วยวิธี ELECTROCHEMICAL BIOSENSOR โดยใช้ HOECHST 33258.
(SEMI-QUANTITATIVE DETECTION OF RAGE cDNA BY ELECTROCHEMICAL BIOSENSOR USING HOECHST 33258) อ. ที่ปรึกษาวิทยานิพนธ์หลัก: รศ.ดร. รัชนา ศานติยานนท์, อ. ที่ปรึกษาวิทยานิพนธ์ร่วม: ผศ.ดร.เทวิน เทนคำเนาว์, 72 หน้า.

ได้นำไบโอเซนเซอร์ทางเคมีไฟฟ้า (electrochemical biosensor) ประยุกต์ใช้ตรวจวิเคราะห์การแสดงออกของยีน β-actin และ ยีน RAGE ในเซลล์เพาะเลี้ยง HeLa และ HepG2 โดยใช้ศักย์ไฟฟ้าประเภท Linear sweep voltammetry เพื่อตรวจวัดจุดสูงสุดของกระแสไฟฟ้า (anodic current peak) และนำผลที่ได้มาเปรียบเทียบกับวิธีดั้งเดิมซึ่งได้แก่ วิธี อะกาโรสเจล อิเล็กโตรโฟริซิส (agarose gel electrophoresis) ขั้นตอนโดยสรุปคือ mRNA จะถูกเปลี่ยนเป็น cDNA และทำการเพิ่มจำนวนโดย PCR หลังจากนั้น PCR product จะถูกตรวจวัดโดยทั้งสองวิธี โดยค่าความแม่นยำของเทคนิคไบโอเซนเซอร์อยู่ในช่วงที่ยอมรับได้ คือยีน β-actin มีค่า CV = 1.88 % สำหรับ 10^4 copies และ 4.68 % สำหรับ 10^9 copies ส่วนยีน RAGE มีค่า CV = 2.25 % สำหรับ 10^9 copies และ 3.74% สำหรับ 10 copies สำหรับเทคนิคไบโอเซนเซอร์ PCR product จะถูกวัดพร้อมกับสารมาตรฐานที่ความเข้มข้นต่างๆ หลังจากนั้นแปลผลจำนวน copy number ของแต่ละยีนจากกราฟมาตรฐานทั้งของวิธี ไบโอเซนเซอร์ และ วิธี อะกาโรสเจล อิเล็กโตรโฟริซิส จากผลการเปรียบเทียบพบว่าทั้งสองวิธีไม่แตกต่างกันอย่างมีนัยสำคัญที่ระดับความเชื่อมั่น 95% โดยมีความสัมพันธ์ y = - 40383.0623 +1.0233 x; p>0.10 ผลการทดลองพบว่าวิธีไบโอเซนเซอร์มีความไวกว่าวิธีอะกาโรสเจล อิเล็กโตรโฟริซิส เพราะสามารถตรวจวัดยีน RAGE ที่มีการแสดงออกปริมาณต่ำๆได้ คือ 10 copies ในขณะที่วิธี อะกาโรสเจล อิเล็กโตรโฟริซิสสามารถมองเห็นที่ปริมาณ 10^4 copies แต่สามารถวัดเชิงปริมาณได้ในช่วงเส้นตรง 10^6- 10^9 copies เมื่อประยุกต์วิธีไบโอเซนเซอร์ทางเคมีไฟฟ้าเพื่อตรวจ ยีน RAGE แบบกึ่งหาปริมาณ พบว่ายีน RAGE ในเซลล์เพาะเลี้ยง HeLa มีการแสดงออกมากกว่ายีน RAGE ในเซลล์เพาะเลี้ยง HepG2 เป็น 2 เท่า โดยมีค่าสัดส่วนยีน RAGE ต่อ ยีน β-actin ของเซลล์ HeLa คือ 0.000905 และ ของเซลล์ HepG2 คือ 0.0004670

ภาควิชา เคมีคลินิก ลายมือชื่อนิสิต ภาริณี กิตติมงคลสุข
สาขาวิชา ชีวเคมีคลินิกและอณูทางการแพทย์ ลายมือชื่อ อ.ที่ปรึกษาวิทยานิพนธ์หลัก รัชนา ศานติยานนท์
ปีการศึกษา 2553 ลายมือชื่อ อ.ที่ปรึกษาวิทยานิพนธ์ร่วม

5277211437 : MAJOR CLINICAL BIOCHEMISTRY AND MOLECULAR MEDICINE
KEYWORDS : ELECTROCHEMICAL BIOSENSOR/ DEP CHIP/ HOECHST 33258/ GENE EXPRESSION/ RAGE/ β- ACTIN

PARINEE KITTIMONGKOLSUK : SEMI-QUANTITATIVE DETECTION OF RAGE cDNA BY ELECTROCHEMICAL BIOSENSOR USING HOECHST 33258. ADVISOR: ASSOC.PROF. RACHANA SANTIYANONT, Ph.D., CO-ADVISOR: ASST.PROF. TEWIN TENCOMNAO, Ph.D., 72 pp.

Electrochemical biosensor has been applied for detection of gene expression of β-actin and RAGE genes. Using linear sweep voltammetry (LSV), β-actin expression in HeLa cell line and RAGE gene expression in HepG2 cell line were detected from the anodic current peak and the results were compared with the conventional agarose gel electrophoresis method. In brief, mRNA was reversed to cDNA and amplified by PCR, the PCR products was subjected to detection either by the electrophoresis or electrochemical biosensor methods. Precision of the biosensor technique was acceptable (β-actin: CV= 1.88 % for 10^4 copies and 4.68 % for 10^9 copies; RAGE: CV = 2.25 % for 10^9 copies, and 3.74% for 10 copies). In biosensor technique, the PCR products were measured in the same run with various concentrations of standard, and copy number of β-actin gene was interpolated from standard curve. Copy number of β-actin gene was then compared between the two techniques. At 95 % confidence limit, the two methods had no significant difference and had significant correlation ($y = -40383.0623 + 1.0233x$; $p>0.10$). Biosensor method was more sensitive than the conventional electrophoresis method because it could detect RAGE gene as low as 10 copies while the conventional method could detect visually at over 10^4 copies and the linearity for semi-quantitative measurement started from 10^6–10^9 copies. When the electrochemical biosensor was applied to detect RAGE gene expression, we found that RAGE gene was expressed twice more in HeLa than HepG2 (relative value of 0.000905 vs. 0.0004670).

Department : Clinical Chemistry Student's Signature Parinee Kittimongkolsuk.
Field of Study : Clinical Biochemistry and Molecular Medicine Advisor's Signature R. Santiyanont.
Academic Year : 2010 Co-advisor's Signature

Acknowledgements

This thesis would not have been possible without the kind support from many people who are gratefully mentioned here.

Above all, I owe my deepest gratitude to my advisor, Assoc. Prof. Dr. Rachana Santiyanont who offered me valuable ideas and suggestions for my thesis. Besides, she pays much attention on my thesis writing and is willing to offer concrete advice at anytime she is available. Her kindness and her support are greatly appreciated. I'm very much obliged to her efforts of helping me complete the thesis.

I'm also extremely grateful to my co-advisor, Asst. Prof. Dr. Tewin Tencomnao for his useful comments and suggestion on this study. He helps me discuss and solve a problem for my research. His patience and kindness are greatly impressive.

In addition, I would like to extend special thanks to ASAHI Glass Grant 2009 and Omics-Nano Medical Technology Development Project, Chulalongkorn University for supporting my research.

Thanks to Mr.Teerapong Lertwittayapon and Miss.Varaporn Rakkhittawatthana for their generous supply of cloned bacteria containing RAGE and β-actin genes.

Special thanks to my family and postgraduate friends, who never failed to give me great encouragement and suggestions.

Contents

Chapter **Page**

Chapter **Page**

List of Tables

List of Figures

Figure **Page**

Figure **Page**

Figure **Page**

Chapter I

Introduction

1.1) Background Information/ Statement of the Problem

Nowadays new technique such as biosensor plays an important role for detection of DNA especially electrochemical biosensor **(1)** because it is easy to invent, rapid, specific, cost effective, less time-consuming, and can detect DNA semi-quantitatively. Although polymerase chain reaction (PCR) using together with agarose gel electrophoresis and real time-PCR techniques are generally used to identify the gene-associated diseases **(2, 3)**, detection of DNA by electrophoresis is time-consuming and can vary upon many factors such as agarose gel quality, or type of running buffer. Moreover, quantitative analysis of the amplification product by real-time PCR technique is very expensive and requires sophisticated instrument and technical skill. So, the electrochemical biosensor technique has been developed to replace gel electrophoresis procedure. Basic biosensor consists of two main parts. First part is the recognition part. Biomolecule that is specific to the target such as nucleic probe is immobilized on the transducer. In this part, the reaction between specific target and immobilizing probe will create the indicated signal that can be detected by the second part. The second part is a transducer that can convert the indicated signal from the previous part to a readable signal such as light or electrical signal **(4, 5)**. The transducer can be modified to gold electrode to increase efficiency of detection **(6, 7)**, or using the electroactive indicator as mediator to transfer electron from the reaction to the electrode, or use DNA intercalator that can bind to DNA and causes change in electron transfer to electrode such as Hoechst 33258 as a label **(8)**. However, all of these methods need difficult steps of immobilizing the DNA probe on the surface of the electrode before hybridization. To reduce immobilization step, the aggregation phenomenon of the target DNA with of Hoechst 33258 to determine presence and absence of DNA in the solution was implemented **(9, 10)**. Hoechst 33258 can bind to minor groove of DNA so, it's more specific to dsDNA than ssDNA.

In this study, we applied electrochemical technique with DNA aggregation induction by Hoechst 33258 to detect commonly expressed gene, β-actin, and

compared its correlation and efficiency with conventional agarose gel technique. Finally, this technique was applied to detect a gene of interest, receptor for advanced glycation endproducts (RAGE). RAGE is a receptor which upon binding to some types of its specific ligands will cause pathological effects in many types of chronic degenerative diseases such as diabetes, atherosclerosis and cancer **(11-14)**. Human liver carcinoma (HepG2) and human cervical cancer (HeLa) cell lines which were previously reported to have RAGE gene expression **(15)** will be used for semi-quantitative detection of RAGE gene expression in this study. Thereafter, the degree of gene expression in both cell lines will be compared by using the relative copy numbers.

1.2) Objectives

1. To semi-quantitatively detect commonly expressed gene, β-actin, by electrochemical biosensor technique and compared its correlation and efficiency with conventional agarose gel technique

2. To apply electrochemical biosensor technique to detect a gene of interest, receptor for advanced glycation endproducts (RAGE)

1.3) Key words: electrochemical biosensor, DEP chip, Hoechst 33258, gene expression, RAGE, β-actin

Chapter II
Literature review

2.1 Technology for gene detection and application

There are several methods to detect DNA.

2.1.1) Conventional agarose gel electrophoresis. This is one of the most well-known tools developed to detect several types of genes. However, it is time-consuming and has low sensitivity because the detection of product depends on gel electrophoresis step that can be varied, not only in type of agarose gel but also in buffer and the applied voltage.

2.1.2) Real time PCR. The technique has been introduced in order to accelerate the speed of detection and enhance process efficiency. Real time PCR is a quantitative determination that can detect a real product at a real exponential phase and can be used to detect chronic disease such as diabetes **(2)** and cancer **(3)**, etc. However, this technique requires a sophisticated instrument and high level of technical skill. Furthermore, chemicals are expensive.

2.1.3) Biosensor technique. This new technology has been applied for detecting nucleic acid, enzyme, antibody, etc. Generally, biosensor consists of two main parts as shown in figure 1. The first part is recognition part. This part contains biological substances that are specific to target analysis such as nucleic acid, enzyme, antibody which are immobilized on the transducer. The second part is transducer which can convert specific signals to readable signals such as light, current or frequency **(4, 5)**.

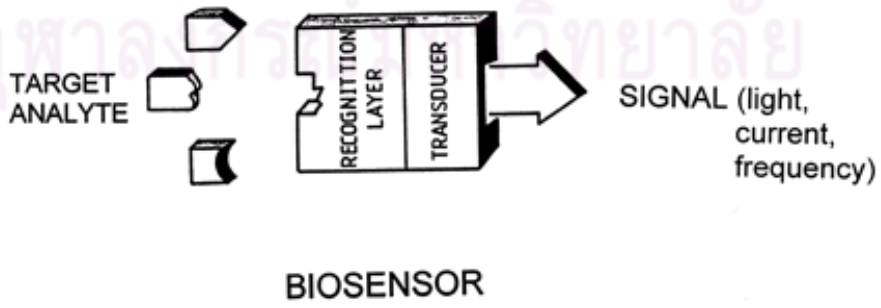

Figure 1 Electrochemical biosensor **(4).**

2.1.3.1) Principle of biosensor. Detection by biosensor consists of three steps. Firstly, the biological substance that is specific to the target is immobilized on

the transducer. Secondly, the target binds specifically to immobilized substance and this is called biological recognition. This part will generate the indicated signal from the reaction such as electron, ion, gas, thermal, light or mass, etc. Finally, the transducer converts indicated signals from step two to readable signals, this step is called physical transduction. The appropriate transducer is an important factor for detecting indicated signals efficiently. For examples, if the indicated signal is an electron, the transducer is an electrode and if the indicated signal is ion, the transducer is ISE (ion selective electrode), etc. In general, good transducer should be sensitive and can response rapidly to indicated signals.

2.1.3.2) The main transducers. Transducers which are used in the biosensor technique are (a) optical biosensor, this technique depends on the optical property such as absorption, transmission, reflection, fluorescence and luminescence; (b) piezoelectric crystal biosensor depends on quartz crystal, the frequency of vibration is affected by mass of a material adsorbed on the surface; and (c) electrochemical biosensor **(16, 17)**, which can be subclassified into three types. The first type is amperometric that measures a change in electric current as a result of electron transferring from sample to the electrode by oxidation or reduction reaction. The second type is potentiometric, a measuring instrument is developed to capture a change in voltage or electric potential, this technique is based on pH or p(ion). The last type is conductimetric in which capture conductivity or change in conductance/ resistance of the solution is measured, but this technique is unpopular **(18, 19)**.

Each type of biosensor can be applied to detect DNA. However, the amperometric biosensor is widely used to detect gene or DNA hybridization or expression than the others. This is because most reactions give an electron directly (depended on redox reaction) and the process is fast and cost-saving **(7, 20-23)**.

2.1.3.3) The electrochemical DNA biosensor or genosensor. The DNA probes that are specific with the DNA target are immobilized on an electrode. The electrode for detecting DNA hybridization mostly uses carbon, gold and mercury electrode **(20)**. However, amalgam, mercury film carbon, and other solid electrodes can also be used as DNA electrode in the DNA hybridization sensors **(24)**. After that, indicated signal that is generated from the hybridization is transduced into a current signal for displaying or analyzing as depicted in figure 2.

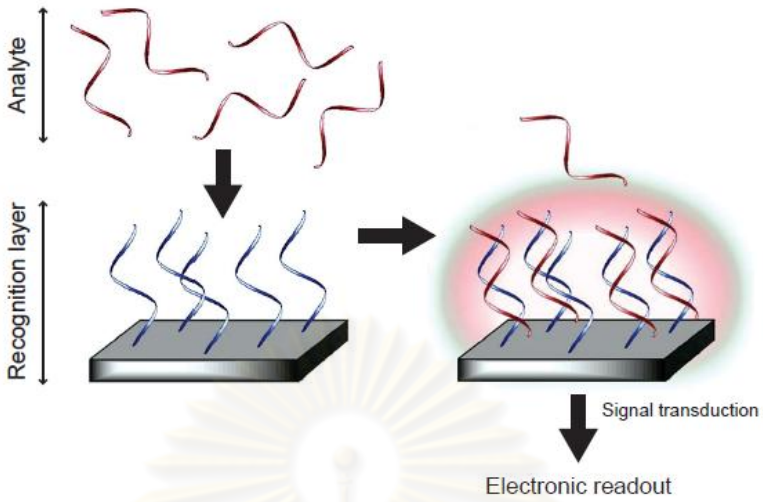

Figure 2 DNA Hybridization of conventional electrochemical DNA biosensor with DNA probes **(21)**.

2.1.3.4) Detection of DNA hybridization with electrochemical biosensor. There are two categoriess **(25)**, the first one is label free or direct detection that depends on the direct guanine oxidation signal (indicator-free), and the second one is label based or indirect detection that is dependent on electroactive hybridization indicator.

A) Label free or direct detection

Guanine residue plays an important role in detecting guanine oxidation signal because it is electrochemical oxidation molecules in DNA that are more reactive than other bases **(26)**. This technique consists of three crucial steps as shown in figure 3, carbon and mercury electrode were used to detect the signal. Regarding those steps, it can be categorized as follows: Immobilization of guanine probe on the electrode, hybridization with complementary target DNA, and detection of the current via guanine oxidation signal by voltammetry.

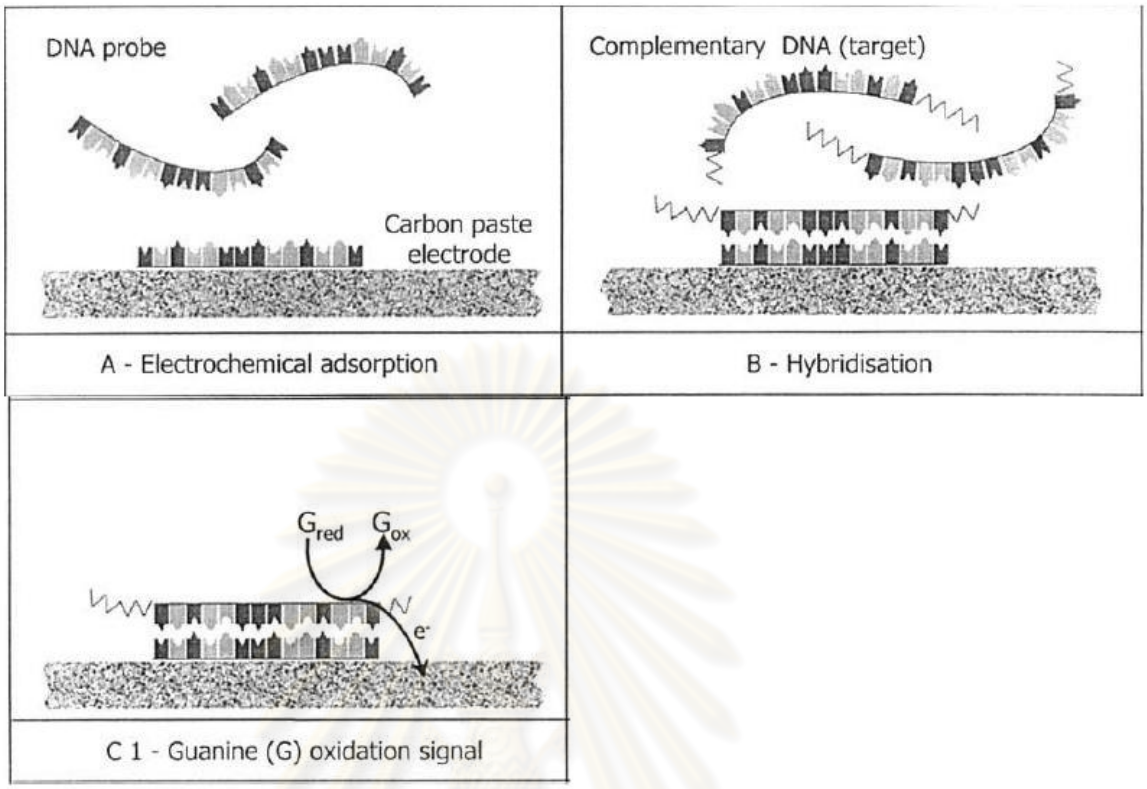

Figure 3 Three steps of electrochemical DNA biosensor detection of guanine oxidation signal **(25).**

The signal decreases when hybridization occurs. This is because guanine in the hybridized form or dsDNA is hidden in duplex structure and hard for the oxidation process to take place while guanine in ssDNA can be oxidized easier **(27, 28)**. However, guanine probes cannot detect its target containing guanine bases because they themselves interfere the guanine probes signal. Thus, inosine-substituted probes (guanine free) that bound to cytosine residue are adopted instead of guanine probes. Consequently, the signal increases after hybridization because the signal depends solely on the target guanine **(29)**. In addition to carbon and mercury electrode, modifying probe to gold can increase the efficiency of hybridization detection and mismatch oligonucleotide **(30)**. As a result, guanine oxidation signal is applied to detect not only DNA hybridization or discrimination between complementary DNA and mismatch DNA **(29)** but also telomerase activity that is a biomarker for cancer cells **(31)**, RNA hybridization for detection of the fecal indicator bacterium *Escherichia coli* for water-quality monitoring **(32)**, apolipoprotein E (apoE) sequences in PCR samples **(33)** and the Catechol-O-methyltransferase (COMT) Val108/158 Met polymorphism that is related to schizopheria **(34)**.

B) Label based or indirect detection

This detection technique is introduced as a better alternative for electrochemical detection. It depends on electroactive indicators for detecting DNA hybridization. It consists of four basic steps; a) immobilization probes (ssDNA) on the electrode, b) hybridization between probes and specific targets, c) reaction between the indicator and dsDNA on the electrode surface, and d) transduction to current via voltametry as illustrated in figure 4. There are many types of indicators as following.

a) Cationic metal complexes

Cationic metal complexes consist of $Co(phen)_3^{3+}$, $Co(bpy)_3^{3+}$, $Fe(bpy)_3^{3+}$, $[Ru(NH3)_6]^{3+}$ and $Ru(bpy)_3^{2+}$, etc **(35-37)**. These indicators are mostly used as mediator for transporting electrons from the guanine oxidation to electrode as shown in figure 5. However, Yang and Thorp **(38)** applied this method to detect trinucleotide Repeat Expansion**.** The currents is detected from the oxidation of the immobilized guanines by $Ru(bpy)_3^{3+}$ that would increase with the number of repeats at tin oxide electrode.

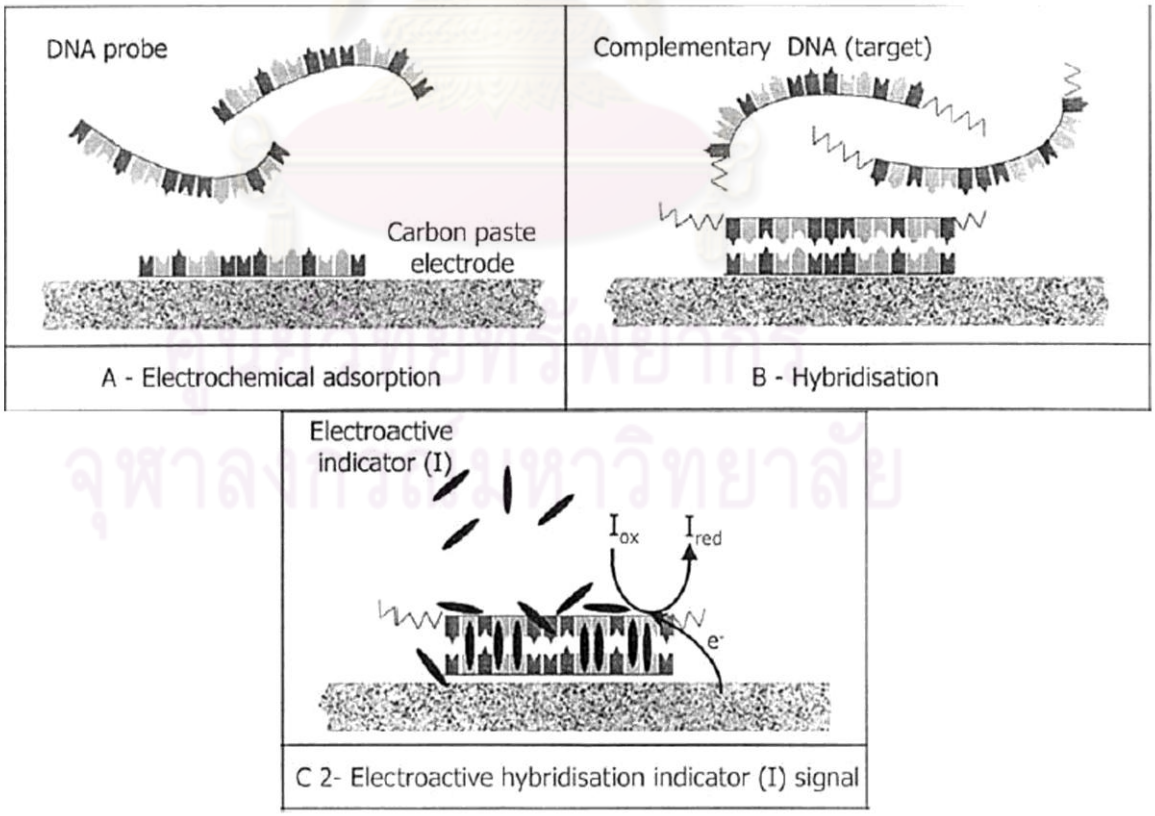

Figure 4 The four steps- indirect detection by using electroactive indicators for detection DNA hybridization **(25).**

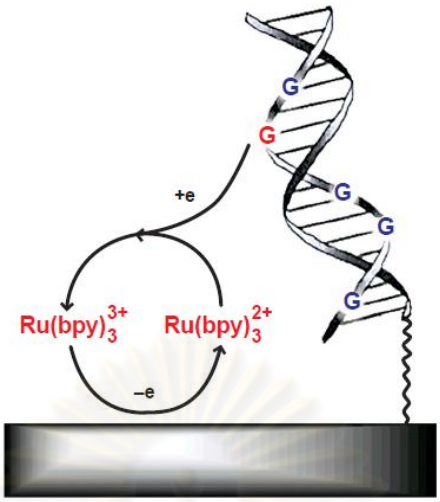

Figure 5 Guanine oxidation mediated by a ruthenium complex in solution in electrochemical DNA biosensor with DNA probes **(21).**

b) DNA intercalators

DNA intercalators are the molecules that can bind DNA in different ways. The properties of intercalator are imperative for high sensitivity gene detection. Various types of intercalators were compared in order to select an appropriate intercalator for the DNA sensor **(1)**.

(a) Organic dyes

Examples of organic dyes are acridine orange and methylene blue. Acridine orange is used to detect hybridization and specific sequences of *Trichoderma harzianum* which is difficult to culture **(39)**. However, the electrochemical signal derived from acridine orange is small and can bind with dsDNA and ssDNA. Thus, this dye has low sensitivity and is not appropriate for discriminating dsDNA from ssDNA. Methylene blue can bind specifically to guanine bases and is used as mediator to transfer electron to the electrode **(40)** or used to distinguish dsDNA from ssDNA using hairpin DNA probe **(41)**. The result shows that methylene blue can bind to dsDNA better than ssDNA or used for gene sequence related to *Trichoderma harzianum* **(42)** and used for recognition of native yeast DNA sequence **(43)**.

(b) Antibiotics

Antibiotics such as daunomycin and mitoxantrone (MXT) are anti-tumor antibiotics. The daunomycin bound to dsDNA by intercalating and bound to ssDNA by electrostatic interactions. It separates the dsDNA from ssDNA by detecting different electrochemical signals. In addition, the electrochemical signal of daunomycin is not influenced by the oxidation derived from oxygen and oligonucleotide probes **(44)**. Daunomycin is applied for detecting the hybridization of DNA and capturing low-molecular weight compounds (toxins, pollutants, drugs) that has affinity for nucleic acids **(18, 45)**. Mitoxantrone can bind tightly to major groove of DNA in reversible redox process in cyclic voltammetry **(46)**.

(c) Bisbenzimide dyes

Example of bisbenzimide dyes is Hoechst 33258, which structure is shown in figure 6.

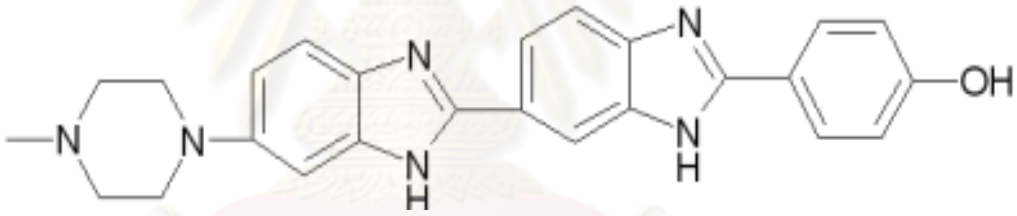

Figure 6 Structure of Hoechst 33258**.**

(http://en.wikipedia.org/wiki/Hoechst_stain; access on 18/09/2553)

Originally, Hoechst 33258 is a fluorescent dye mostly used to detect DNA or tracking DNA replication **(47)**. It can bind effectively within a minor groove **(48, 49)** of double strand DNA at A-T rich region (figure 7) **(48, 50-52)**.

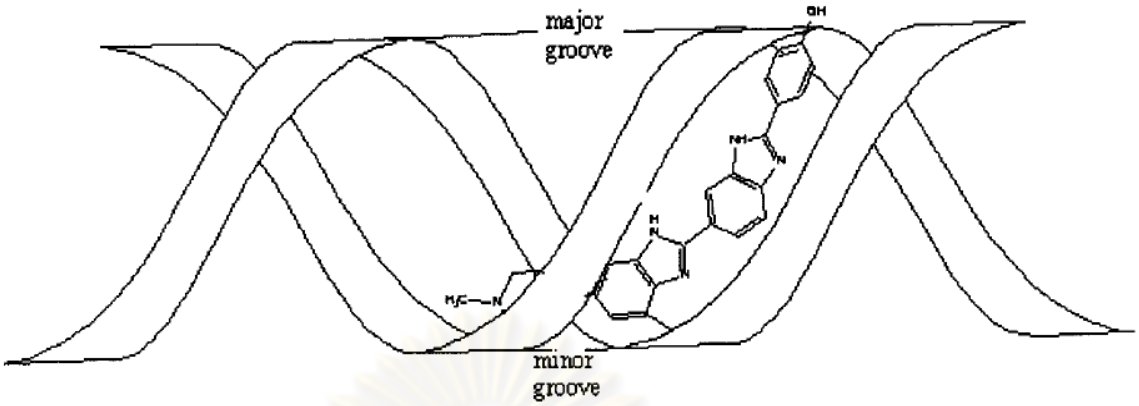

Figure 7 Hoechst 33258 binding to minor groove of DNA **(53).**

In the electrochemical detection, electrochemically active dye plays an important role. In the free form, it is oxidized on the electrode to give an electron to produce electrochemical signal which can be measured as anodic current peak **(8, 53)**. The anodic current peak is measured via linear sweep voltammetry (LSV). This dye is widely used to detect hybridization of the interested gene or DNA **(1, 54)** because it can bind to dsDNA more specific than ssDNA according to minor groove property. The anodic signal will decrease when hybridization occurs comparing to without DNA in the solution. In addition electrode can be modified to gold to increase efficiency **(55)**.

However, all of the electrochemical biosensors that were mentioned above require immobilizing step of capturing probe on the electrode which is difficult to prepare and time-consuming. Kobayashi, et al. **(9)** has developed electrochemical DNA biosensor for DNA quantification without immobilizing probe on the electrode. This help reducing time and cost by using Hoechst 33258 as a redox active compound to aggregate with DNA that was previously amplified by polymerase chain reaction (PCR). The Hoechst 33258 is commonly used because the effect of DNA aggregation by this molecule is better than the others **(56)**. The anodic current signal was measured by linear sweep voltammetry (LSV) and was reversely proportional to DNA concentration. In other words, if there is a large number of DNA in the solution, the anodic current signal will decrease because there is a small amount of free Hoechst 33258 left in the solution. On the other hand, if the amount of DNA in the solution is low, the anodic current peak will increase as shown in figure 8.

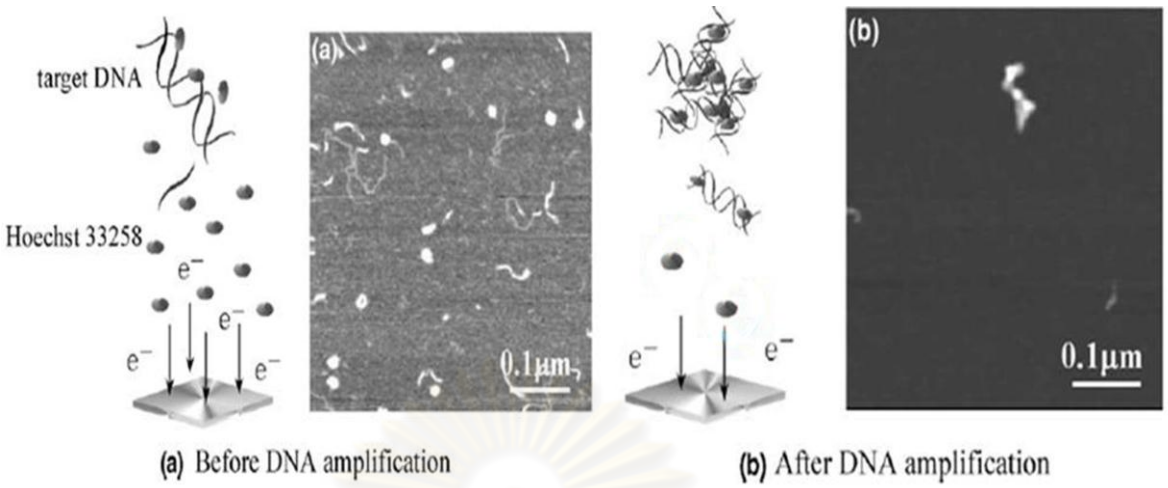

Figure 8 Electrochemical DNA biosensor without immobilizing probe using Hoechst 33258 **(9)**.

The electrochemical biosensor using Hoechst 33258 has been applied for detecting DNA in many areas such as detection of bovine constituents in feedstuff **(10)**, detection of single nucleotide polymorphisms (SNPs) of clinically important alleles by using disposable electrochemical printed (DEP) chip as demonstrated in figure 9 **(57)**, identification of meat species by using DEP chips with loop mediated isothermal amplification technique **(58)**. The electrochemical biosensor aggregated with Hoechst 33258 is easy to use, cheap, and helpful in reducing time of testing because it eliminates immobilizing step which can reduce operating expenses for specific probes. Moreover, when it is used in conjunction with PCR, it can increase the efficiency of detection.

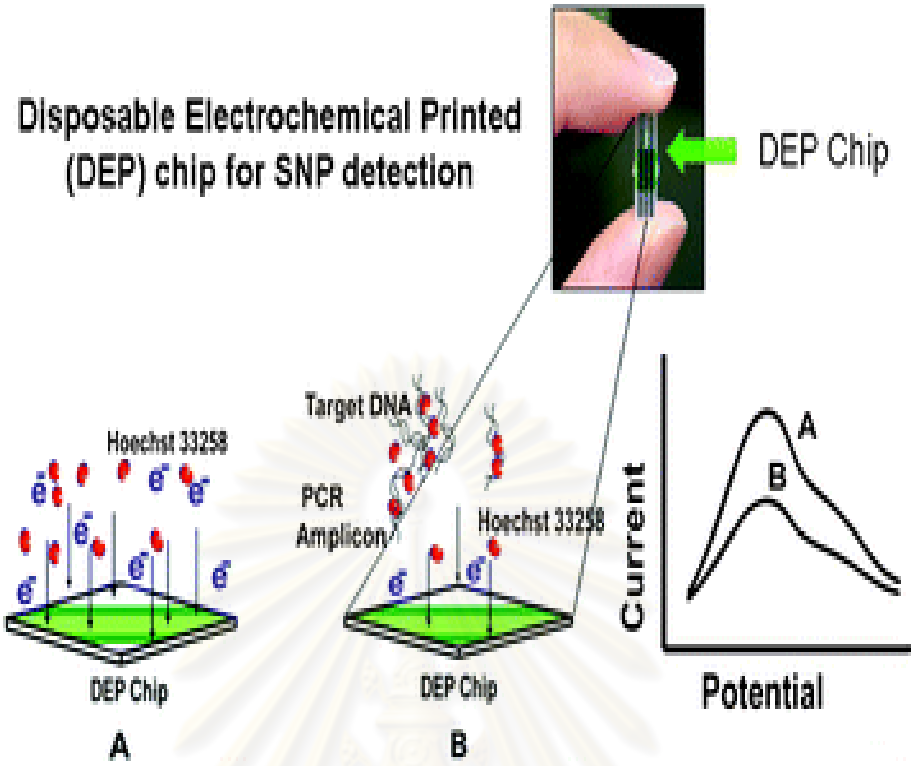

Figure 9 Disposable Electrochemical Printed (DEP) chip for SNP detection **(57)**.

However, most of the electrochemical biosensor techniques are applied to detect DNA hybridization with electroactive indicator. In this study, we has modified the label-free electrochemical biosensor by using disposable electrochemical printed (DEP) chip, Hoechst 33258, and linear sweep voltammetry (LSV) for semi-quantitative detection of gene expression. The technique will be modified to detect commonly expressed gene, β-actin, that is a housekeeping gene and compare its correlation and efficiency with conventional agarose gel electrophoresis technique. Finally, this technique is applied to detect a gene of interest, receptor for advanced glycation endproducts (RAGE), which is a receptor which upon binding to some types of its specific ligands will cause pathological effects in many types of chronic degenerative diseases

2.2 Receptor for Advanced Glycation Endproducts (RAGE)

RAGE is a member of the immunoglobulin superfamily of cell surface molecules which locates on chromosome 6 in the MHC class III region **(59)**. The full RAGE receptors consist of 5 domains. The first domain is cytosolic domain or

cytoplasmic tail which is responsible for signal transduction. The second one is transmembrane domain which anchors the receptor in the cell membrane. The third is variable domain which binds the RAGE ligands, and the last two parts are constant domains (figure 10).

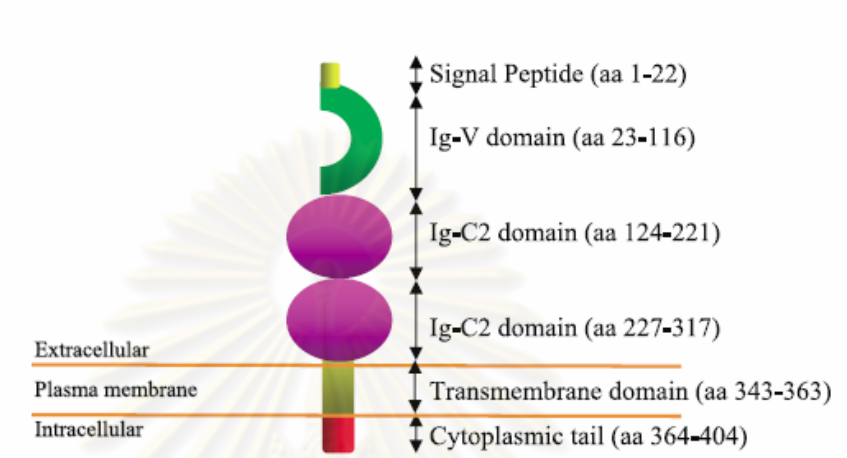

Figure 10 Schematic representation of RAGE. Domains of RAGE are shown with corresponding amino acid numbers **(60)**.

The full length RAGE cDNA consists of 11 exons. RAGE can occur in many isoforms as a result of alternative splicing **(61)**. The spliced forms lead to change in the protein coding region of RAGE, for example, protein changes in the ligand-binding domain of RAGE or the removal of the transmembrane domain and cytosolic tail. In human lung and cultured aortic smooth muscle cells, there are 19 naturally occurring RAGE splicing. Most of the alternative spliced form is RAGEv1 and it is named as esRAGE or soluble RAGE (sRAGE) **(60, 62, 63)**. However, the most abundantly expressed form of RAGE in lung tissues and smooth muscle cells is full length. In human brain, there are three established RAGE isoforms **(64)** such as full length RAGE (RAGE), secretory RAGE (sRAGE), and N-truncated RAGE (NtRAGE), but the most abundant form of RAGE in the hippocampus is RAGEv1 .

RAGE is normally found as surface receptor in endothelial cells, vascular smooth muscle cells, leukocyte, macrophages, the nervous system, lungs, muscles, peritoneum and the kidneys. RAGE is normally expressed at low levels in most tissue except lung **(65)**. It can bind to multiligands **(66, 67)**; such as advanced glycation end-products (AGEs) **(68)**, amphoterin or HMGB1 **(69)**, S100/calgranulin family **(70)**,

Mac-1 (αMβ2,CD11b/CD18) or leukocyte integrin **(71)** and Amyloid-β-protien **(72, 73)**. Upon binding to its ligands, AGE can trigger signal transduction that leads to pathogenesis. RAGE implicates with various chronic pathologies depend on its ligand **(74)** such as diabetes, inflammation **(75)**, cancer, macrovascular disease, Alzheimer's disease (AD) or amyloidoses **(76)**. Ligands of RAGE and the associated pathophysiological settings are shown in figure 11.

Ligand for receptor for AGE	Physiologic/ pathophysiologic impact
Advanced glycation endproducts	Diabetes, renal failure, amyloidoses, (e.g. CML-adducts) inflammation, oxidant stress, aging
Amyloid-b peptide and b sheet fibrils	Alzheimer' s disease, amyloidoses
S100/ calgranulins	Development, neurite outgrowth inflammation, tumour biology

Figure 11 RAGE ligands and their pathophysiological state **(68)**.

2.2.1) Advanced Glycation Endproducts (AGEs)

This is the common ligand for RAGE. Normally, AGEs are usually formed in hyperglycemia especially in diabetic condition **(14)**, prolonged inflammation, aging and oxidative stress condition **(77)**. They are formed through three pathways as illustrated in figure 12.

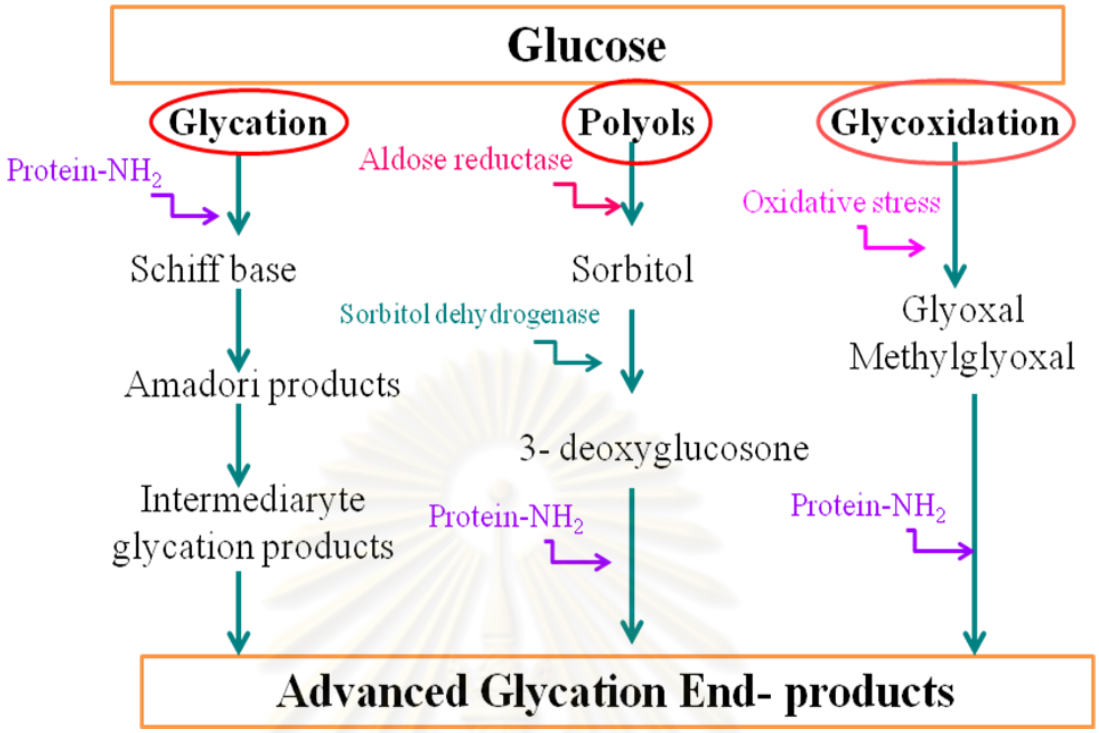

Figure 12 Diagram of advanced glycation end product (AGE) formation**(14)**.

The first pathway is glycation pathway. This pathway depends on glucose concentrations, time and temperature. There are several steps of AGE formation. Glucose will bind with protein and form Schiff base. Then, it will be transformed into Amadori products and to intermediary glycation products before becoming AGEs. The second pathway is polyols pathway in which the glucose is transformed by adolase reductase to sorbitol. Then, sorbital is converted to 3-deoxyglucosone by sorbitol dehydrogenase. After that, protein will bind with the intermediate product to form AGE and the last pathway is glycoxidation, which depends on oxidative stress and leads to form glyoxal and methylglyoxal which are unstable, so, they can rapidly react with protein and form AGE.

AGEs- RAGE interaction (78)

The mechanism is reduction in endothelial nitric oxide synthase (eNOS) that results in nitric oxide (NO) reduction; activation of nicotinamide dinucleotide phosphate (NAD(P)H) oxidase which catalyzes the chemical reaction and provides reactive oxygen species (ROS); activation of RAS p21 which is a GDP/GTP binding G protein that leads to activation of MAP kinase signaling; activation of P38 mitogen-

activated protein kinases (p38 MAP kinase) ; and activate cell division cycle 42 protein (Cdc 42) to activate Rac which is a subfamily of the Rho family of GTPases and small (~21 kDa) signaling G proteins. The latter four pathways can activate transcription factor such as nuclear transcription factors (NF-κB) to increase transcription of endotheli, intercellular adhesion molecule-1 (ICAM-1), vascular adhesion molecule-1 (VCAM-1), vascular endothelial growth factor (VEGF), Interleukin-6 (IL-6), tumor necrotic factor (TNF-α) and RAGE. All of the proteins cause functional and structural changes manifestations which lead to symptoms of diabetic vascular complications **(79)** as shown in figure 13.

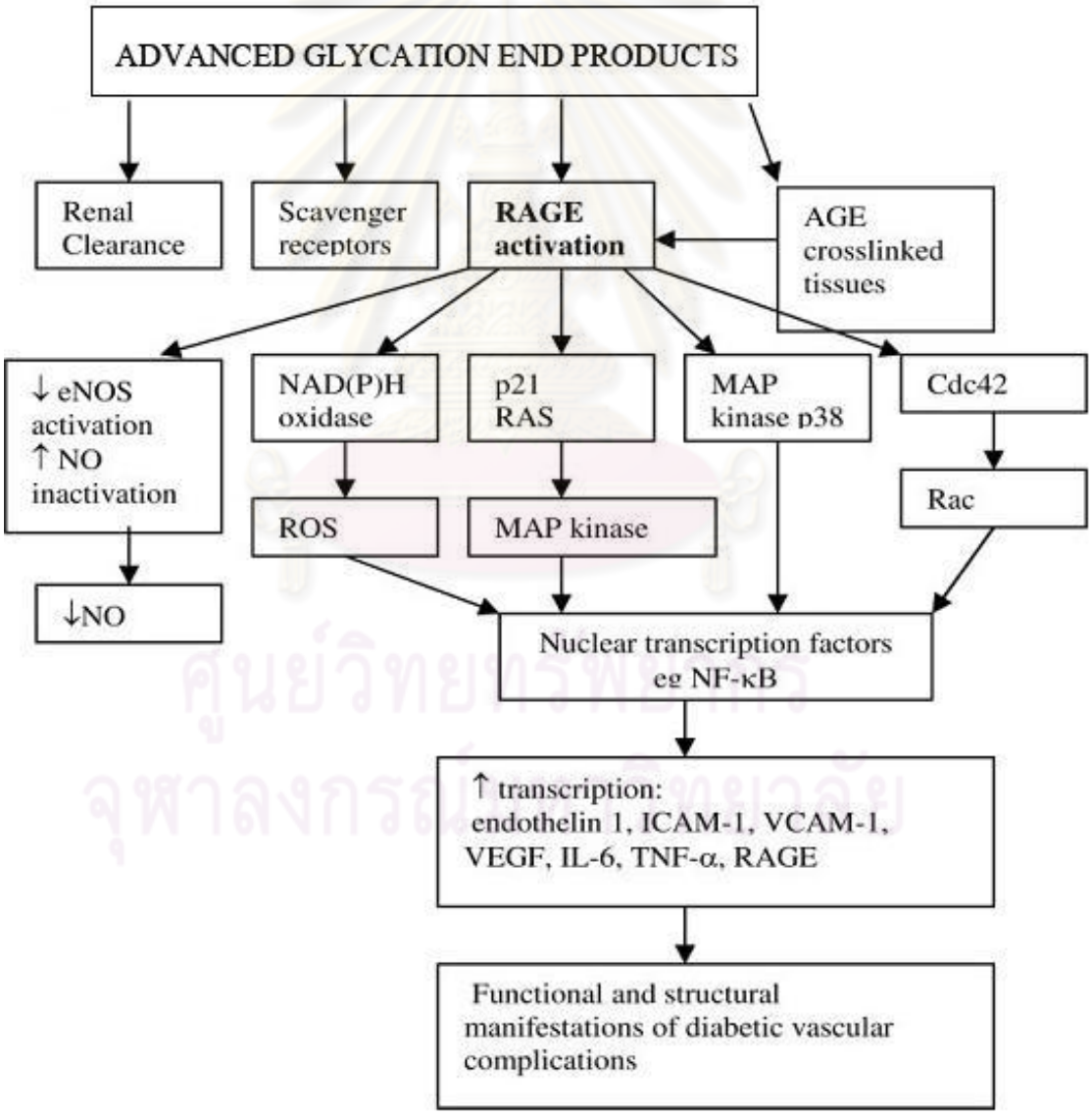

Figure 13 Effects of AGEs-RAGE interaction **(79)**.

AGE binds to RAGE in diabetes complication alters cellular properties especially in vascular homeostasis **(11)** and causes many implication such as atherosclerosis **(12, 80)**, cardiovascular disease **(81)**, renal glomerulus **(82)** and inflammation **(83, 84)**.

2.2.2) Amphoterin (HMGB1) ligand

Amphoterin (HMGB1) ligand or a high-mobility group box1 is a nonhistone chromosomal DNA-binding protein. It is normally found in nucleus.

HMGB1- RAGE interaction

Amphoterin is released by necrotic cell **(85)** acting as a mediator in tissue injury and inflammation **(86, 87)**. In addition, amphoterin is expressed and secreted by cancer cells. It causes cellular activation and results in increase expression of cytokine and growth factor, NF-κB. In tumor, the HMGB1 is implicated in tumor formation, progression and metastasis. High level of HMGB1and RAGE appear in several solid tumor implicate with metastasis tumors **(88)** except for corresponding tumor tissue of non-small cell lung cancer that expresses RAGE at low level **(89)**. Thus, the HMGB1-RAGE axis is related to inflammation and cancer **(90)**. In addition, the RAGE-amphoterin reaction plays an essential role in the migration of monocytes through the endothelium **(91)**.

2.2.3) S100/ calgranulin family ligand

S100 proteins has a low molecular weight (~11 kDa) that can bind with calcium via EF hand motifs **(92)**. An EF-hand is a helix-loop-helix motif that coordinates Ca^{2+} binding. It is expressed in vertebrates exclusively, display a cell-specific distribution, and regulate a large variety of intracellular activities such as cell proliferation, differentiation and shape, membrane trafficking, Ca^{2+} homeostasis, protein phosphorylation, transcription, cytoskeleton dynamics. S100 proteins consist of many members **(93)** especially, S100A11 and S100B which is secreted from astrocytes and neuron **(94, 95)**. They are the best characterized proteins **(96).**

S100/ calgranulin family- RAGE interaction (97)

S100A11 binding with RAGE stimulates inflammation-induced chondrocyte hypertrophy **(80, 87, 98)**. S100B binding with RAGE leads to neuronal survival **(99,**

100) neurite extension1, neuronal injury or apoptosis **(101),** stimulation of IFN-γ-inducible protein expression in monocytes3 **(102)**. In addition, S100 protein family such as S100P has been shown to mediate tumor growth, drug resistance, and metastasis through RAGE binding because S100P is specifically expressed in cancer cells in adults. So, blocking S100P-RAGE interaction shows effective therapy for cancer **(103, 104)**

2.2.4) MAC-1or leukocyte integrin

MAC-1 (αMβ2, CD11b/CD18) was originally described as a cell surface marker for macrophages **(105)**. Mac-1 plays roles in inflammatory process and contributes to emigration from the vessel **(106)**. The recruitment of leukocytes from the circulation into surrounding tissues at sites of inflammation or injury requires multisteps; step one , adhesive and signalling events; step two, including selectin-mediated capture and rolling; step three, leukocyte activation; step four, integrin-mediated firm adhesion and step five, their subsequent transendothelial migration **(107)**.

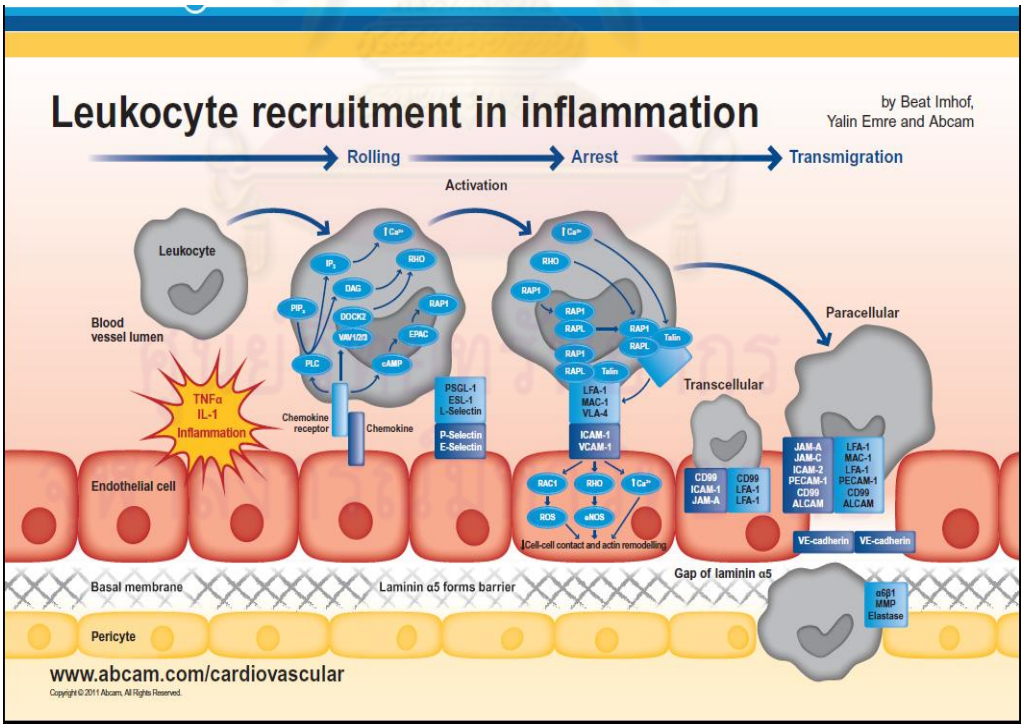

Figure 14 Leukocyte recruitment in inflammation **(108)**

MAC-1or leukocyte integrin- RAGE interaction

the RAGE–Mac-1 interaction related to leukocyte migration. In vitro, RAGE-dependent leukocyte adhesion to endothelial cells is mediated by a direct interaction of RAGE with the β2-integrin (Mac-1) involving in the transcription factor NF-κB **(109)** and the interaction is increased by the proinflammatory RAGE-ligand such as ligand, S100-protein. So, The RAGE– Mac-1 interaction is a novel pathway of leukocyte recruitment relevant in inflammatory disorders associated with increased RAGE expression **(71).**

2.2.5) Amyloid-β-peptide (Aβ) and β-sheet fibrils ligand

Amyloid-β-peptide composes of 39-43 amino acids. It is neurotoxic and induces oxidative stress in endothelial cells **(110)**. Excessive accumulation of Aβ in central nervous system (CNS) leads to Alzheimer's disease **(111)**.

Amyloid-β-peptide-RAGE interaction (73, 112)

This interaction leads to the transportation of amyloid β across the blood- brain barrier (BBB) into central nervous system (CNS) and expression of proinflammatory cytokines and endothelin-1. To confirm the role of RAGE in BBB transportation of Aβ, the homogenous RAGE null mice were studied **(80)**. The result found that the BBB transport of Aβ was invisible in RAGE null mice **(72)** so RAGE was related to transportation of Aβ across BBB.

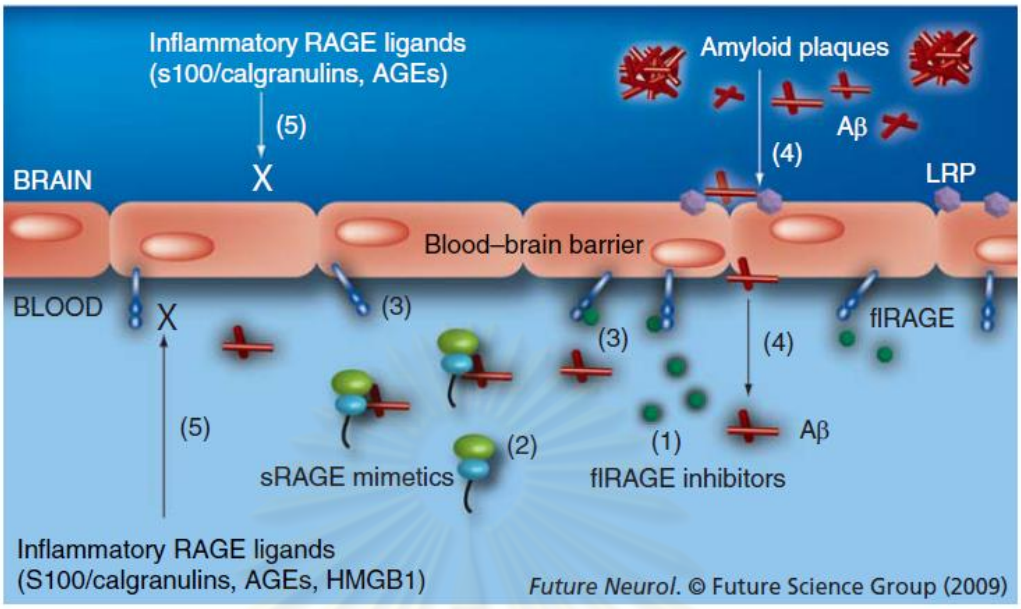

Figure 15 Potential strategy to prevent RAGE activation in Alzheimer's disease across blood–brain barrier **(112).**

Figure 15 suggests that adding RAGE inhibitors (item 1), or sRAGE mimetics (item 2) into the circulation will reduce full length RAGE activation by endothelial cells at the blood–brain barrier (step 3) and promote Aβ transport from brain to the periphery by Low-density lipoprotein-related protein (LRP-1) (step 4). This will reduce the effects of other RAGE inflammatory ligands (S100/calgranulins and AGEs) in the brain and circulation (step 5).

In conclusion, RAGE is related to pathology because it can bind to multiligands such as AGE, HMGB1, S100 family, Mac-1and Aβ protein and cause signaling induction of the deleterious cascades. The RAGE variants occur from alternative splicing and RAGE variants from each organ are different. In addition, there are many studies supporting that the soluble RAGE has an ability to neutralize AGE actions **(113)** or can be used as therapeutic targets for cardiovascular diseases **(114)**, reduced risk for AD **(112),** coronary artery disease, and hypertention **(115-118)**.

Chapter III
Materials and Methods

3.1) Materials

Equipments	Manufacturers, Country
1) -20 ^{o}C Freezer	Sanyo Electric, Japan
2) -80 ^{o}C ULT Deep Freezer	IlShin Lab, Korea
3) 4 ^{o}C Refrigerator	Sharp, Japan
4) Analytical Balance	Mettler Toledo, Switzerland
5) Auto pipette	Gilson, France
6) Block heater	Wealtec, USA
7) Cell Culture Flask (25 cm^2)	SPL Life Sciences, Korea
8) Centrifuge tube 15, 50 ml	Corning, USA
9) CO_2 incubator	Sheldon Manufacturing, USA
10) DEP chip (SP-P and EP-N model)	BioDevice Technology, Japan
11) DNA Chip Tester	BioDevice Technology, Japan
12) Disposable Serological pipette (5, 10 ml)	Corning, USA
13) Electrophoresis power supply	Bio-Rad, USA
14) Gel documentation (Gel Doc) systems	Syngene, UK
15) Gel Electrophoresis Apparatus	Bio-Rad, USA
16) Glasswares	Pyrex, USA
17) Microcentrifuge	Denver Instrument, USA
18) Microcentrifuge tubes (1.5 ml)	Bio-Rad, USA
19) NanoDrop (UV-Visible Spectrophotometer)	Bioactive, USA
20) PCR tubes	Bioscience, USA

21) Six-well plates	Corning, USA
22) Syringe filter	Corning Life Sciences, USA
23) Thermal Cycler (PTC-200)	MJ Research, USA
24) Vacuum Concentrator (DNA SpeedVac)	Thermo Electron, USA
25) Vortex Mixer	Finepcr, Korea
26) Water Bath	Memmert, Germany

Chemicals	**Manufacturers, Country**
1) Agarose gel	Research Organics, USA
2) Ampicillin	Atlantic, Thailand
3) Bacto tryptone	Biobasic, Canada
4) Diethyl pyrocarbonate (DEPC)	Sigma Aldrich, USA
5) DNA ladder 100 bp	Fermentas, Canada
6) Dulbecco's modified Eagle's medium (DMEM)	HyClone, USA
7) EDTA-Trypsin 0.25% (1X)	HyClone, USA
8) Ethanol	Merck, Germany
9) Ethidium bromide	Sigma Aldrich, USA
10) Fetal bovine serum (FBS)	HyClone, USA
11) Maxiprep kit	Invitrogen, USA
12) NucleoSpin® RNA II	Macherey-Nagel, Germany
13) Phosphate buffered saline (PBS)	HyClone, USA
14) Potassium phosphate (Monobasic, anhydrous)	Biobasic, Canada

15) Potassium phosphate (Dibasic, anhydrous)	Biobasic, Canada
16) Primer	Pacific Science, France
17) Taq DNA polymerase kit	Fermentas, Canada
18) Tri-RNA Reagent	Farvogen, Taiwan
18) Verso cDNA synthesis kit	ABgene, UK
19) Yeast extract	Biobasic, Canada

3.2) Methods

The methods used in this study can be divided into five parts according to the diagram below.

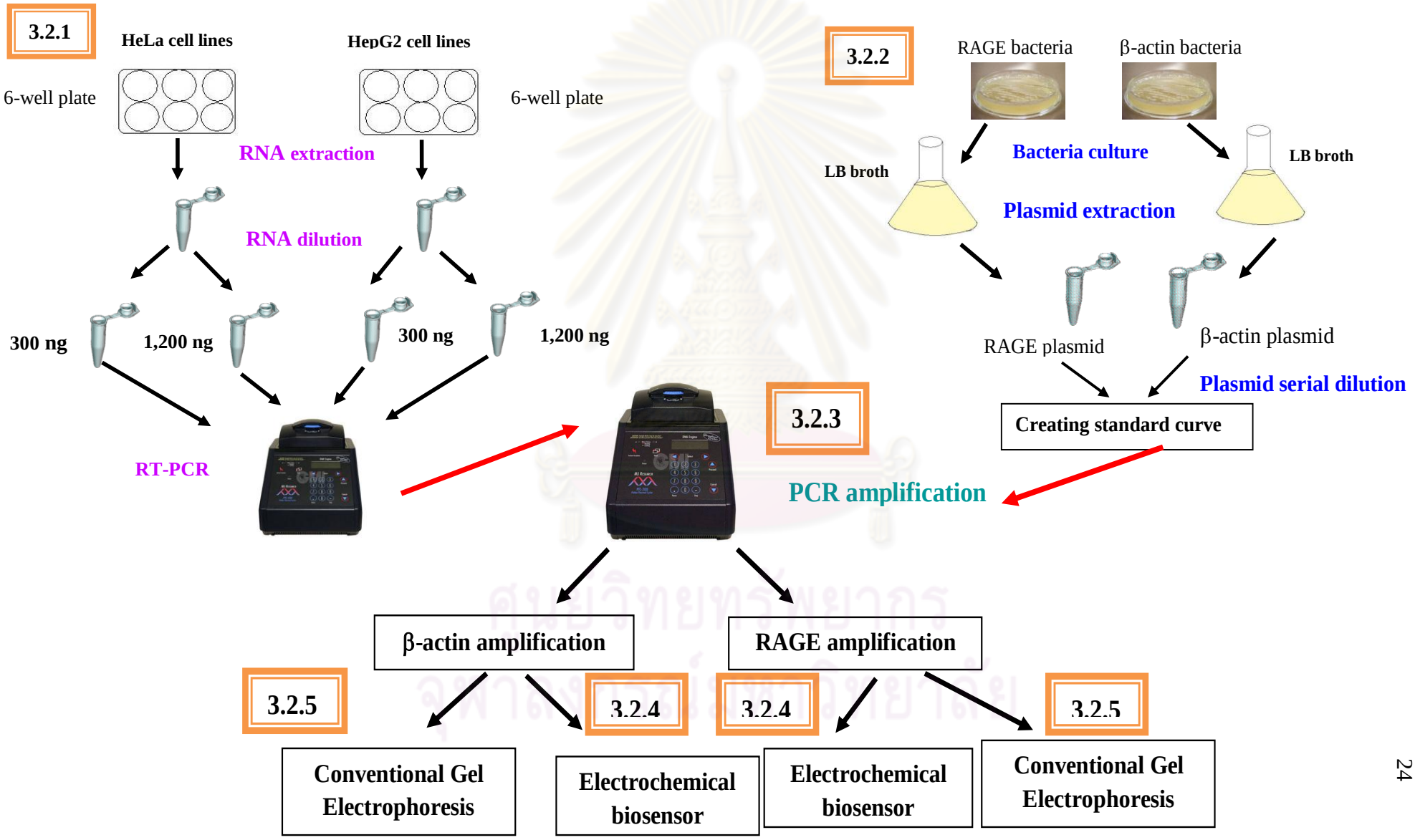
3.2.1
HeLa cell lines
HepG2 cell lines
6-well plate
6-well plate
RNA extraction
RNA dilution
300 ng
1,200 ng
300 ng
1,200 ng
RT-PCR
3.2.2
RAGE bacteria
β-actin bacteria
LB broth
Bacteria culture
LB broth
Plasmid extraction
RAGE plasmid
β-actin plasmid
Plasmid serial dilution
Creating standard curve
3.2.3
PCR amplification
β-actin amplification
RAGE amplification
3.2.5
3.2.4
3.2.4
3.2.5
Conventional Gel Electrophoresis
Electrochemical biosensor
Electrochemical biosensor
Conventional Gel Electrophoresis

3.2.1) Extraction of RNA and RT-PCR amplification

HeLa and HepG2 cell lines were cultured in 25 sq.cm flasks with 10% FBS DMEM at 37 °C under 5% CO_2. Then, HeLa and HepG2 cells were seeded in six-well plate at a cell density of 1×10^6 cells/well in complete growth medium, incubated overnight at 37 °C under 5% CO_2, and total RNA was extracted by two techniques. The first technique is Tri-RNA reagent and the second is nucleospin RNA II kit, then RNA concentration was measured by NanoDrop. For Tri-RNA protocol, firstly, wash cells 2 times with 1X PBS, then, add Tri-RNA reagent 1 ml, then transferred 1 mL of cell suspension to 1.5 ml new tube. Add 200 µl chloroform, mix by inversion and vortex. Then, incubate at room temperature for 15 minutes. After that, centrifuged the mixture at >12,000 x g for 15 minutes at 4 ºC and carefully removed the supernatant into a 1.5 ml new tube, add 500 µl cold isopropanol into the supernatant tube and gently mixed by inversion. Then, incubate at -20 ºC for 30 minutes and centrifuged the mixture at >12,000 x g for 15 minutes at 4 ºC. Removed and discarded the supernatant and dried by placing the top of the tube on RNASE free paper. Then, resuspended the RNA pellet in 1 mL 70% ethanol. (RNA from this step can be kept for 1 year at -20 ºC). Centrifuged the mixture at >7,500 x g for 5 minutes at 4 ºC, removed and discarded the supernatant. Air-dried the pellet by placing the top of the tube on RNase free paper for 30 minutes and speed vac for 1 minute. Then, resuspended RNA pellet in 30 µl RNase-free water (DEPC treated water). After that, incubated at 65 ºC for 10 minutes and stored RNA at -20 ºC or - 80 ºC. For RNA isolation by commercial kit, the method was as described by the manufacturer's manual **(119)**. Cells were lysed by incubation in a lysis buffer that contains large amounts of chaotropic ions in order to inactivate RNases. The lysis buffer created appropriate binding conditions which favored adsorption of RNA to the silica membrane. Contaminating DNA which also bound to the silica membrane was removed by an rDNase solution which was directly applied onto the silica membrane during preparation. Simple washing steps with two different buffers removed salts, metabolites and macromolecular cellular components and pure RNA was finally eluted under low ionic strength conditions with RNase-free water. Then, total RNA from two techniques were diluted to two concentrations of

300 ng/µl and 1,200 ng/µl. Then, RNA was reversed to cDNA in a total volume of 20 µl per reaction by Verso cDNA synthesis kit at 42 °C 30 min for 1cycle, and inactivation at 95 °C 2 min for 1 cycle.

3.2.2) Creating standard curves for RAGE and β-actin genes

RAGE and β-actin fragments were cloned into pcDNA3.1/V5-His TOPO TA expression kit and pGEM-T easy vector kit. The total sizes (inserted cDNA + plasmid vector) were 6,764 bp and 3,671 bp respectively. The recombinant plasmid were transformed into *E.coli*. Then, the bacteria containing cloned RAGE and β-actin plasmids were cultured in Lysogeny broth (LB) or Luria broth, incubated overnight at 37^{o}C with vigorous shaking. After that, plasmids were extracted by Maxiprep kit. The extracted plasmids were checked by gel electrophoresis and the right plasmid was used to make a 10-fold dilution for making 5 concentrations of standards. RAGE standards were 10^9, 10^7, 10^5, 10^3, and 10 copies and β-actin standards were 10^9, 10^8, 10^7, 10^6, 10^5 and 10^4 copies to cover the applicable concentrations from samples. Various standard concentrations will be amplified by PCR in the same run of the samples and used for creating standard curves with agarose gel electrophoresis and electrochemical biosensor methods.

For standard calculation

Standard concentrations were calculated according to Applied Biosystems **(120)**

1. Calculate the mass of a single plasmid molecule

$$m = [n][1.096\text{e-}21 \frac{g}{bp}]$$

where: n = plasmid size (bp)
m = mass
e-21 = $\times 10^{-21}$

Note: Plasmid size is plasmid + insert

2. Calculate the mass of plasmid containing the copy number of interest

Copy # of interest × mass of single plasmid = mass of plasmid DNA needed

For example

Copy of interest is 10^9 copies × mass from step one = mass of plasmid DNA

3. Calculate the concentrations of plasmid DNA needed to achieve the copy number of interest. Divide the mass needed (calculated in step 2) by the volume to be pipette into each reaction.

In this example, 5 µl of plasmid DNA solution was pipetted into each PCR reaction.

Copy #	Mass of plasmid DNA needed (g)		Final concentration of plasmid DNA (g/µL)
300,000	4.92e-12	÷ 5 µL	9.84e-13
30,000	4.92e-13		9.84e-14
3,000	4.92e-14		9.84e-15
300	4.92e-15		9.84e-16
30	4.92e-16		9.84e-17

4. Prepare a serial dilution of the plasmid DNA by using following formula

$$C_1V_1 = C_2V_2$$

3.2.3) Polymerase chain reaction (PCR) amplification

Since non-specific PCR product can interfere DNA detection by electrochemical DNA biosensor, the design of specific primers is necessary.

3.2.3.1) Design specific primers for RAGE gene depends on RAGE specificity and % A-T.

1. Exon 1-3, product size 332 bp

Forward 5’- AGC AGT TGG AGC CTG GGT G- 3’

Reverse 5’- GGA CTC GGT AGT TGG ACT TGG - 3’

% A+T = 40.06

2. Exon 4-7, product size 383 bp

Forward (RAGE F1) 5’ – GTGGGGACATGTGTGTCAGAGGGAA - 3’

Reverse (RAGE R1) 5’ - TGAGGAGAGGGCTGGGCAGGGACT -3’

% A+T = 38.38

Product size 216 bp

Forward (RAGE F1) 5’ – GTGGGGACATGTGTGTCAGAGGGAA - 3’

Reverse (RAGE R2 inner) 5’-

TGGGCTGAAGCTACAGGAGAAGGTG -3’

% A+T = 41.20

3.2.3.2) Primer for β-actin gene, product size 656 bp

Forward 5’- ACGGGTCACCACACTGTGC- 3’

Reverse 5’- CTAGAAGCATTTGCGGTGGACGATG - 3’

% A+T = 46.0

3.2.3.3) Optimization of PCR conditions

RAGE gene

1**) Condition for first primers, product size 332 bp**:

1200 ng RNA of HeLa and HepG2 cell lines were used to test the condition. The PCR tube contained 10X *Taq* Buffer, **1.5 mM $MgCl_2$**, 10 mM dNTPs , 10 µM primers and 1.25 U *Taq* DNA polymerase under PCR conditiion of pre-denaturation at 95 °C 5 min, denaturation at 95 °C 30 sec, annealing between 50-59 °C for 30 sec, extension at 72 °C 30 sec, and post extension at 72 °C 5 min.

2) **Condition for F1 and R1 primers (product size 332 bp) and F1 and R2 primers (product size 216 bp).**

The experiments were done in two conditions.

2.1) 10X *Taq* Buffer, **1.5 mM $MgCl_2$** (1.5 mM $MgCl_2$ for β- actin), 10 mM dNTPs, 10 µM primers and 1.25 U *Taq* DNA polymerase under PCR conditiion of pre-denaturation at 95 °C 5 min, denaturation at 95 °C 30 sec, annealing temperature optimization between 59-63 °C for 30 sec, extension at 72 °C 30 sec, and post extension at 72 °C 5 min.

2.2) 10X *Taq* Buffer, **1.0 mM $MgCl_2$** (1.5 mM $MgCl_2$ for β- actin), 10 mM dNTPs, 10 µM primers and 1.25 U *Taq* DNA polymerase under PCR conditiion of pre-denaturation at 95 °C 5 min, denaturation at 95 °C 30 sec,

annealing temperature optimization between 59-63 °C for 30 sec, extension at 72 °C 30 sec, and post extension at 72 °C 5 min.

β- actin

Condition for β- actin contained 10X *Taq* Buffer, **1.5 mM $MgCl_2$**, 10 mM dNTPs, 10 µM primers and 1.25 U *Taq* DNA polymerase and amplification condition was pre-denaturation at 95 °C 5 min, denaturation at 95 °C 30 sec, annealing temperature optimization between 58-61 °C for 30 sec, extension at 72 °C 45 sec and post extension at 72 °C 15 min.

3.2.4) RNA concentration and PCR condition for electrochemical biosensor

The samples were amplified for 30 cycles by Thermal Cycler in 50 µl reaction mixture. For RAGE gene, the PCR mixture composed of 5 µL cDNA of either 300 ng or 1200 ng that reached concentration to 75 ng/ 5 µl and 300 ng/ 5 µl respectively. Each PCR reaction contained 10X *Taq* Buffer, 1.0 mM $MgCl_2$ (1.5 mM $MgCl_2$ for β-actin), 10 mM dNTPs , 10 µM primers and 1.25 U *Taq* DNA polymerase under PCR conditiion of pre-denaturation at 95 °C 5 min, denaturation at 95 °C 30 sec, annealing at 65 °C 30 sec, extension at 72 °C 30 sec, and post extension at 72 °C 5 min. The β- actin amplification condition was pre-denaturation at 95 °C 5 min, denaturation at 95 °C 30 sec, annealing at 58 °C 30 sec, extension at 72 °C 45 sec and post extension at 72 °C 15 min. The same concentration of cDNA from HeLa and HepG2 were used for amplification of both RAGE and β- actin genes.

3.2.5) Electrochemical biosensor detection

3.2.5.1) Optimization of conditions for detection. Stock solution (200 µM) of Hoechst 33258, [2-(4-hydroxyphenyl) -5- (4-methyl-1-piperazinyl) -2,5 – bi (1H-benzimidazole)] was prepared by dissolving Hoechst 33258 in high purity distilled water which has been filtered through 0.2 µm syringe filter, then divided into small aliquots and kept in the dark at -20 °C. Appropriate phosphate-buffered saline (PBS) concentration and pH were tested with 25, 50, 100 and 200 mM at pH 6.4, 7.4 and 7.8. Just before use, Hoechst 33258 stock solution was diluted in various PBS and then mixed with negative PCR products and positive PCR product

(10^9 copies) to reach the final Hoechst 33258 concentration of 20 µM. The mixture was incubated in heat box at 37°C for 25 sec, and then 20 µl was loaded on working electrode of the disposable electrochemical printed (DEP) chips both SP-P and EP-N model in figure 16 and measured by biosensor device as shown in figure 17. The results from using two DEP models were compared.

Figure 16 Disposable electrochemical printed (DEP) chips (A) square working electrode SP-P model and (B) round working electrode EP-N model (http://www.biodevicetech.com/products/depchip/dep_ep.shtml access on18/09/2553).

Figure 17 (A) biosensor device and (B) biosensor connector

Both SP-P and EP-N model consist of three electrodes which are working electrode, reference electrode and counter electrode, but there are different shapes of working electrode. SP-P chip model consists of square carbon working electrode of area 3.04 mm^2 and EP-N chip model consists of round carbon working electrode of area 2.64 mm^2. The detection program is multichannel DNA chip tester (measurement program) using linear sweep voltammetry (LSV) as shown in figure 18, scan rate is 100 mV/s, initial electric potential was 1,000 mV, and final electric potential was 1000 mV. The changes in anodic current were recorded and anodic current peak was

used for further calculation. The appropriate concentration of Hoechst 33258 was selected between 20 µM and 50 µM**.**

Linear sweep voltammetry (LSV)

The voltage change from v1 to a value v2 (linear increase with time).

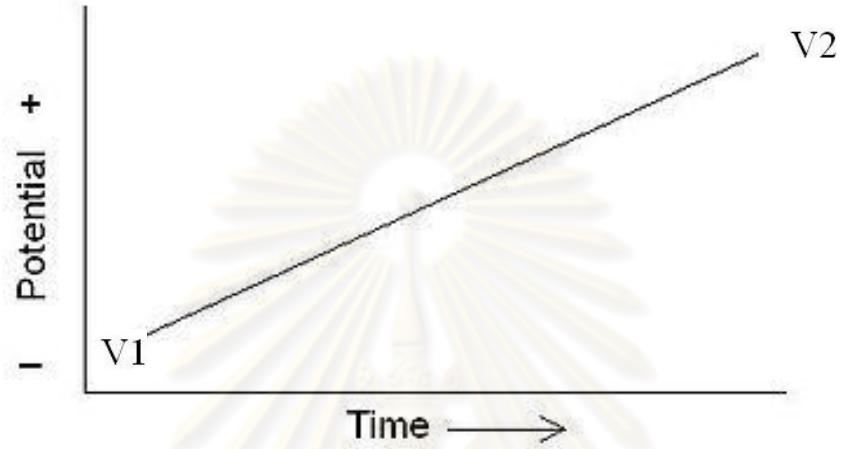

Figure 18 Linear sweep voltammetry (LSV)

3.2.5.2) Precision of electrochemical biosensor method.

The precision of electrochemical biosensor method was evaluated using β-actin gene and RAGE gene at two concentrations. For within day, the β-actin DNA standards were tested at low level (10^4 copies) and high level (10^9 copies) and measured repeatedly for 10 times. Likewise, RAGE DNA standards were tested at low level (10 copies) and high level (10^9 copies) and measured repeatedly for 10 times in a single day. For between day precision study, the β-actin DNA standards were tested at low level (10^4 copies) and high level (10^9 copies) and measured repeatedly for 3 times a day for 10 days. Likewise, RAGE DNA standards were tested at low level (10 copies) and high level (10^9 copies) in the same manner.

3.2.6) Electrophoresis detection of DNA

PCR products of RAGE and β- actin from the same tubes that have been used for electrochemical biosensor detection were loaded on 2% agarose gel and run in 1X Tris-acetate and EDTA (TAE) buffer with 90 V for 35 min. The agarose gel was stained with ethidium bromide and specific bands measured with Gel Documentation (Gel Doc) system.

3.2.7) Comparison between electrochemical biosensor technique and agarose gel electrophoresis technique. To detect commonly expressed gene, β-actin, by electrochemical biosensor technique and compared its correlation and efficiency with conventional agarose gel technique. HeLa and HepG2 cDNA both at 300 ng and 1200 ng were amplified for β-actin gene by PCR. Each cDNA dilution from two cell lines was measured in triplicate (n=12). After that, PCR product from the same tubes were detected by electrochemical biosensor and conventional agarose gel electrophoresis. Then, the copy numbers of β-actin gene were determined from electrochemical biosensor and agarose gel electrophores to compare sensitivity and the correlation between two techniques.

Electrochemical biosensor aggregation with Hoechst 33258 was applied for detection of RAGE gene from HeLa and HepG2 by using cDNA from the same tube of β-actin gene amplification. The copy number of RAGE gene was interpolated from standard curve and RAGE gene expression was calculated in relative to β-actin gene. When different concentrations of cDNA were used, the relative values or estimated RAGE cDNA concentration from HeLa and HepG2 were analyzed by paired t-test.

Chapter IV

Results

4.1) Optimization of PCR condition

4.1.1) The first primers (product size 332 bp).

The RAGE primers were checked for specificity with NCBI primer blast program. Although these primers have high A-T percentage, they can amplify several of genes as illustrated in figure 19.

Detailed primer reports

Primer pair 1

	Sequence (5'->3')	Length	Tm	GC%
Forward primer	AGCAGTTGGAGCCTGGGTG	19	56.30	63.16%
Reverse primer	GGACTCGGTAGTTGGACTTGG	21	54.26	57.14%

>NM_172197.1 Homo sapiens advanced glycosylation end product-specific receptor (AGER), transcript variant 2, mRNA

```
product length = 290
Forward primer  1    AGCAGTTGGAGCCTGGGTG  19
Template        39   ...................  57

Reverse primer  1    GGACTCGGTAGTTGGACTTGG  21
Template        328  .....................  308
```

>NM_001136.3 Homo sapiens advanced glycosylation end product-specific receptor (AGER), transcript variant 1, mRNA

```
product length = 332
Forward primer  1    AGCAGTTGGAGCCTGGGTG  19
Template        39   ...................  57

Reverse primer  1    GGACTCGGTAGTTGGACTTGG  21
Template        370  .....................  350
```

>XR_115124.1 PREDICTED: Homo sapiens hypothetical LOC100508411 (LOC100508411), partial miscRNA

```
product length = 208
Forward primer  1     AGCAGTTGGAGCCTGGGTG  19
Template        1748  GTTG.......G.....G.  1766

Forward primer  1     AGCAGTTGGAGCCTGGGTG  19
Template        1955  .....A...CC........  1937
```

>XR_109406.1 PREDICTED: Homo sapiens hypothetical LOC100506609 (LOC100506609), partial miscRNA

```
product length = 208
Forward primer  1     AGCAGTTGGAGCCTGGGTG  19
Template        1748  GTTG.......G.....G.  1766

Forward primer  1     AGCAGTTGGAGCCTGGGTG  19
Template        1955  .....A...CC........  1937
```

>XR_111719.1 PREDICTED: Homo sapiens hypothetical LOC100508411 (LOC100508411), partial miscRNA

```
product length = 208
Forward primer  1     AGCAGTTGGAGCCTGGGTG  19
Template        1748  GTTG.......G.....G.  1766
```

Figure 19 The designed RAGE primers are specific for various genes.

When RNA from two cell lines were amplified RAGE gene in the same run with RAGE cDNA standard under condition 1.5 mM Mg^{2+} and annealing temperature at 50 °C, the result shows that HeLa and HepG2 cell line have two non specific bands so this condition cannot be used for amplification RAGE gene (figure 20).

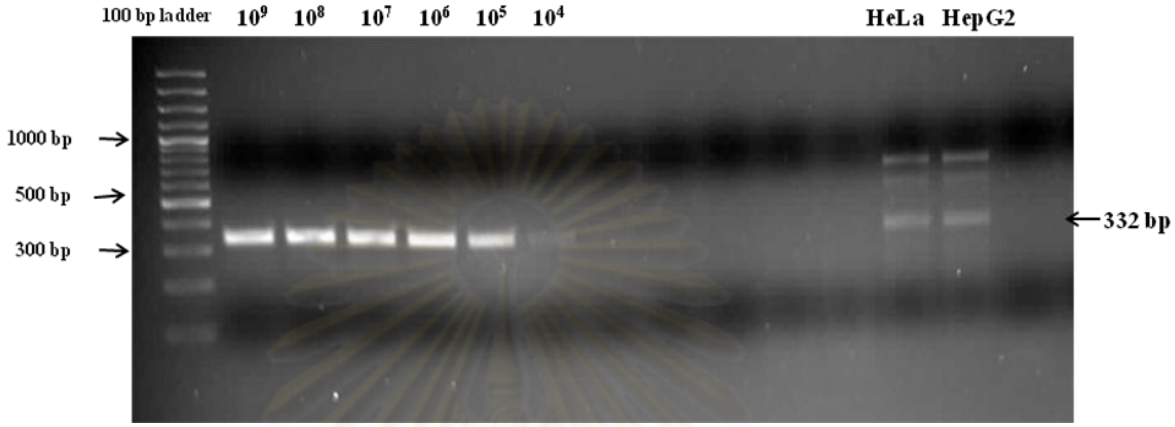

Figure 20 RAGE gene amplification for RAGE cDNA standard and HeLa and HepG2 RNA

4.1.1.1) Optimization of annealing temperature under condition of 1.5 mM Mg^{2+}

The annealing temperature gradient at 50 °C, 53 °C, 56 °C and 59 °C were used to optimize annealing temperature as shown in **figure 21**.

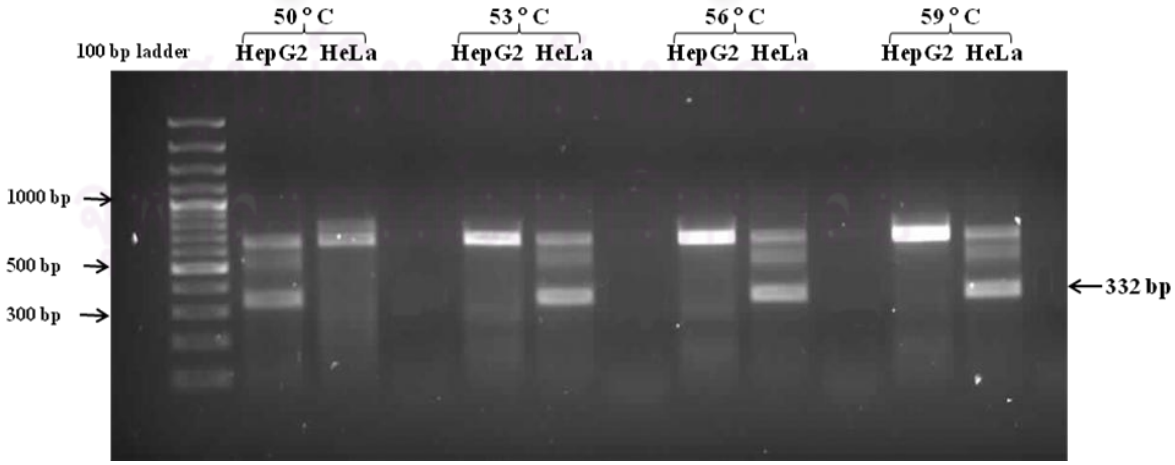

Figure 21 PCR products obtained when the annealing temperature gradient at 50 °C, 53 °C, 56 °C and 59 °C were used for HepG2 and HeLa respectively.

From the results, there were two non specific bands found at all the temperatures used, so these cannot as well be used for amplification of RAGE gene. Thus, these primers are not suitable for RAGE gene amplification and design of the new primers was done.

4.1.2) F1 and R1 primers (product size 383 bp).

These primers are specific for major variants of RAGE, both variant one and two (figure 22).

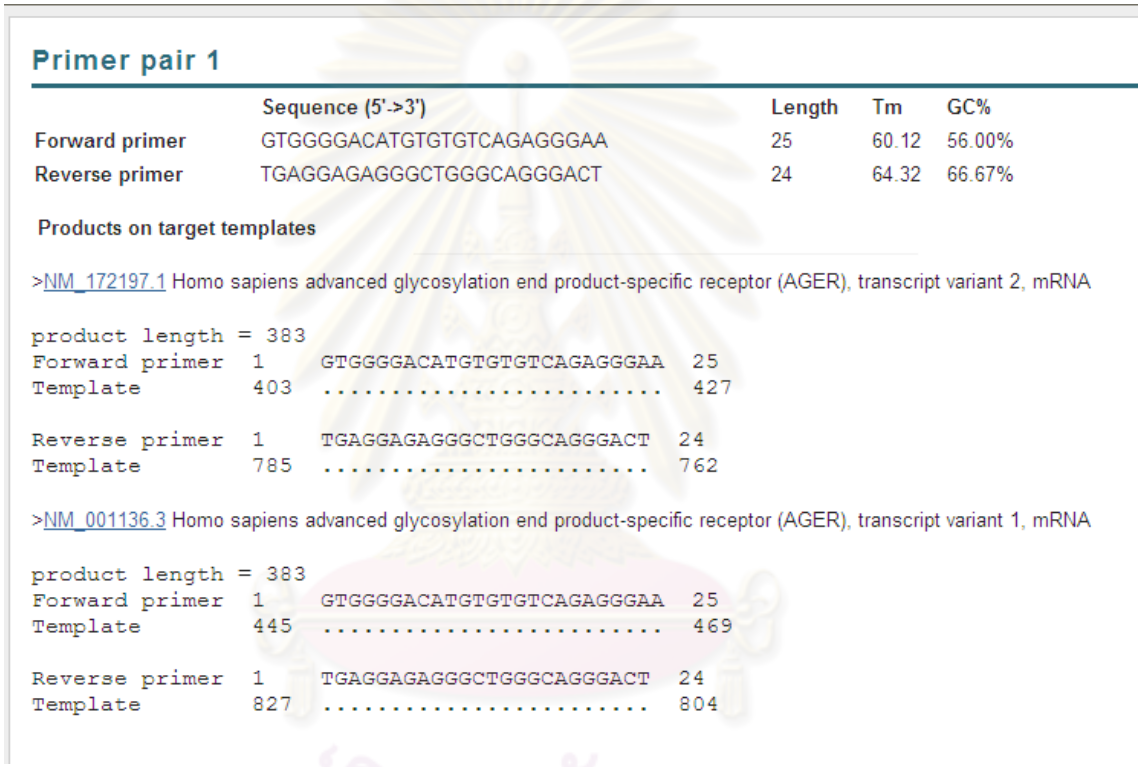

Primer pair 1

	Sequence (5'->3')	Length	Tm	GC%
Forward primer	GTGGGGACATGTGTGTCAGAGGGAA	25	60.12	56.00%
Reverse primer	TGAGGAGAGGGCTGGGCAGGGACT	24	64.32	66.67%

Products on target templates

>NM_172197.1 Homo sapiens advanced glycosylation end product-specific receptor (AGER), transcript variant 2, mRNA

```
product length = 383
Forward primer  1    GTGGGGACATGTGTGTCAGAGGGAA  25
Template        403  .........................  427

Reverse primer  1    TGAGGAGAGGGCTGGGCAGGGACT  24
Template        785  ........................  762
```

>NM_001136.3 Homo sapiens advanced glycosylation end product-specific receptor (AGER), transcript variant 1, mRNA

```
product length = 383
Forward primer  1    GTGGGGACATGTGTGTCAGAGGGAA  25
Template        445  .........................  469

Reverse primer  1    TGAGGAGAGGGCTGGGCAGGGACT  24
Template        827  ........................  804
```

Figure 22 Blast for RAGE primers, F1 and R1 shows specificity for variants 1 and 2.

4.1.2.1) Optimization of annealing temperature under condition of 1.5 mM Mg^{2+}

The range of annealing temperature was 62 °C – 66 °C. From the result, there was two non-specific bands all the temperature that means cannot use these conditions as shown in figure 23.

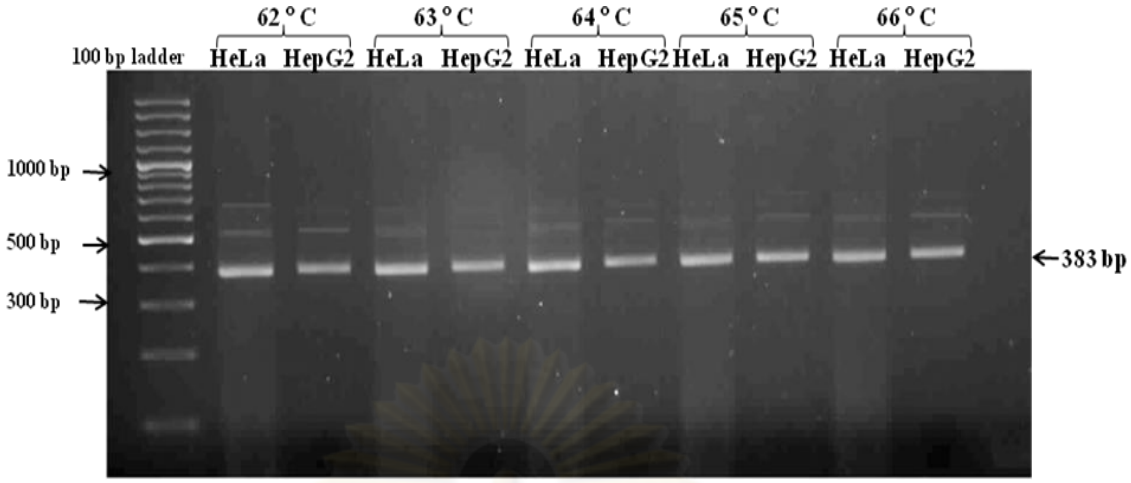

Figure 23 RAGE gene amplification of HeLa cell line and HepG2 cell line at 62 °C, 63 °C, 64 °C, 65 °C and 66 °C respectively.

4.1.2.2) Optimization of annealing temperature under condition 1.0 mM Mg^{2+}

The range of annealing temperature was 63°C – 66 °C. At 63 and 64 °C, two faded non-specific bands were detected whereas at 65 °C and 66 °C gave one specific band (figure 24). However the temperature at 65 °C is better because the band at 65 °C is sharper than at 66 °C.

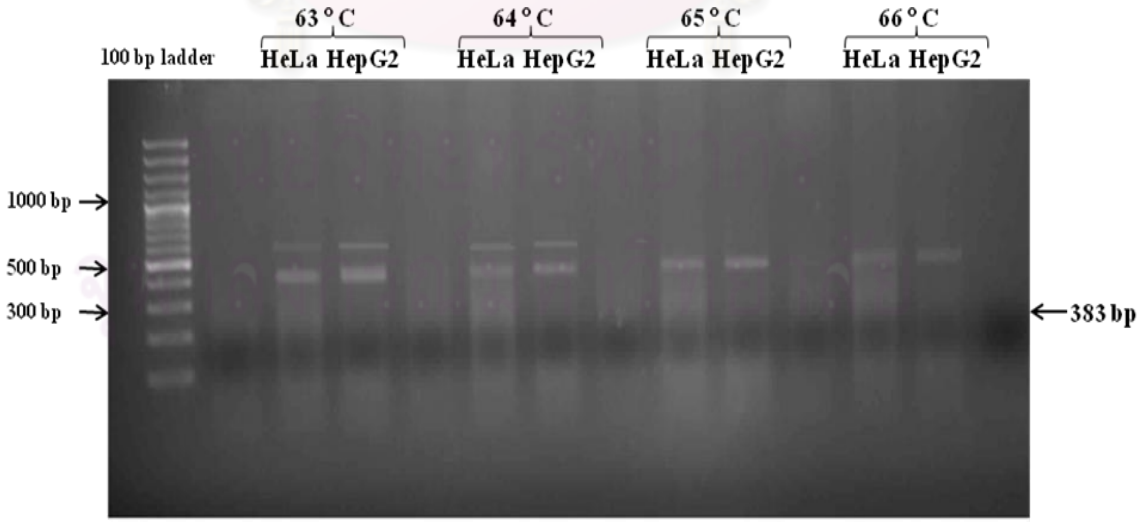

Figure 24 RAGE gene amplification of HeLa cell line and HepG2 cell line at 63 °C, 64 °C, 65 °C and 66 °C respectively.

4.1.3) F1 and R2 primers (product size 216 bp).

Similar to F1 and R1 primer, F1 and R2 primer are specific for amplification of both RAGE variants one and two (figure 25).

Primer pair 1

	Sequence (5'->3')	Length	Tm	GC%
Forward primer	GTGGGGACATGTGTGTCAGAGGGAA	25	60.12	56.00%
Reverse primer	TGGGCTGAAGCTACAGGAGAAGGTG	25	59.95	56.00%

Products on target templates

>NM_172197.1 Homo sapiens advanced glycosylation end product-specific receptor (AGER), transcript variant 2, mRNA

```
product length = 216
Forward primer  1    GTGGGGACATGTGTGTCAGAGGGAA  25
Template        403  .........................  427

Reverse primer  1    TGGGCTGAAGCTACAGGAGAAGGTG  25
Template        618  .........................  594
```

>NM_001136.3 Homo sapiens advanced glycosylation end product-specific receptor (AGER), transcript variant 1, mRNA

```
product length = 216
Forward primer  1    GTGGGGACATGTGTGTCAGAGGGAA  25
Template        445  .........................  469

Reverse primer  1    TGGGCTGAAGCTACAGGAGAAGGTG  25
Template        660  .........................  636
```

Figure 25 Blast for F1 and R2 primers showed specificity for RAGE variants 1 and 2.

4.1.3.1) Optimization of annealing temperature under condition of 1.5 mM Mg^{2+}

The range of annealing temperature was 62 °C – 66 °C. Two non-specific bands were observed at all the temperature tested (figure 26).

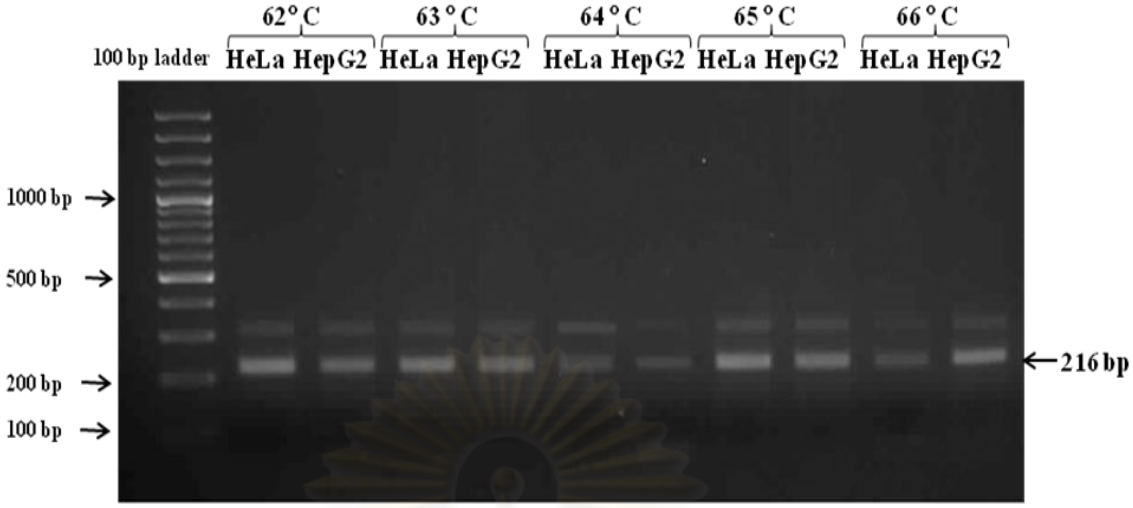

Figure 26 RAGE gene amplification with F1 and R2 primers of HeLa cell line and HepG2 cell line at 62 °C, 63 °C, 64 °C, 65 °C and 66 °C showed non specific amplification.

4.1.3.2) Optimization of annealing temperature under condition of 1.0 mM Mg^{2+}

The range of annealing temperature was 61 °C – 65 °C. From the result, there were two non-specific bands at 61- 64 °C whereas amplification at 65 °C gave one specific band (figure 27).

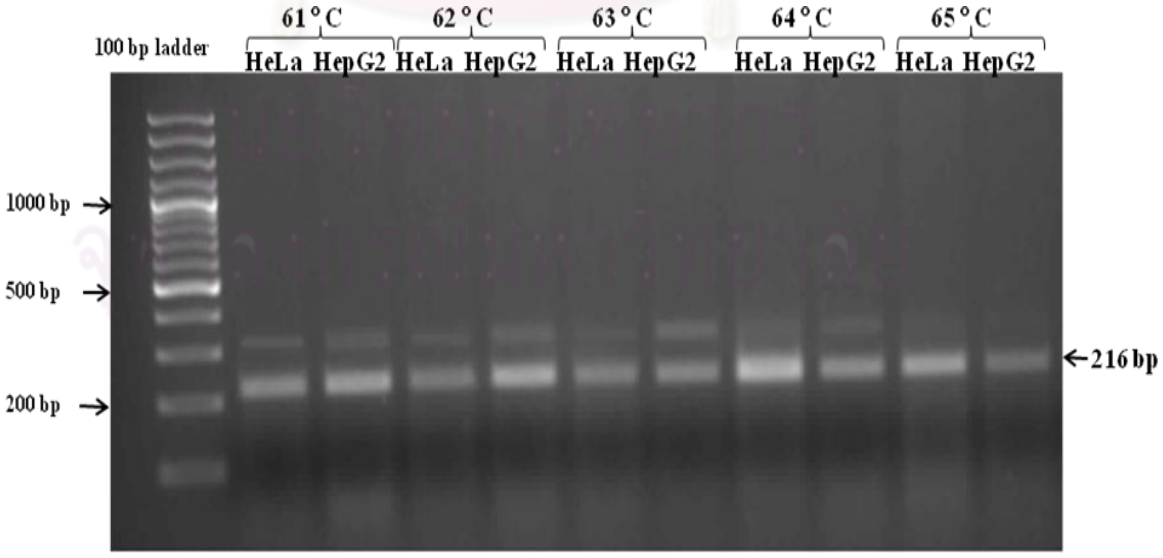

Figure 27 RAGE gene amplification with F1 and R2 primers of HeLa cell line and HepG2 cell line at 61°C-65°C.

From condition of F1 and R1 primers and F1 and R2 primer, the proper annealing temperature is 65 °C so RNA of HeLa and HepG2 were amplified by two primer sets to choose the best primer set. The results in figure 28 showed that at 65 °C annealing temperature, F1 and R1 primers were better than F1 and R2 primers because the former gave specific amplified RAGE gene product. Thus, F1 and R1 primers were used.

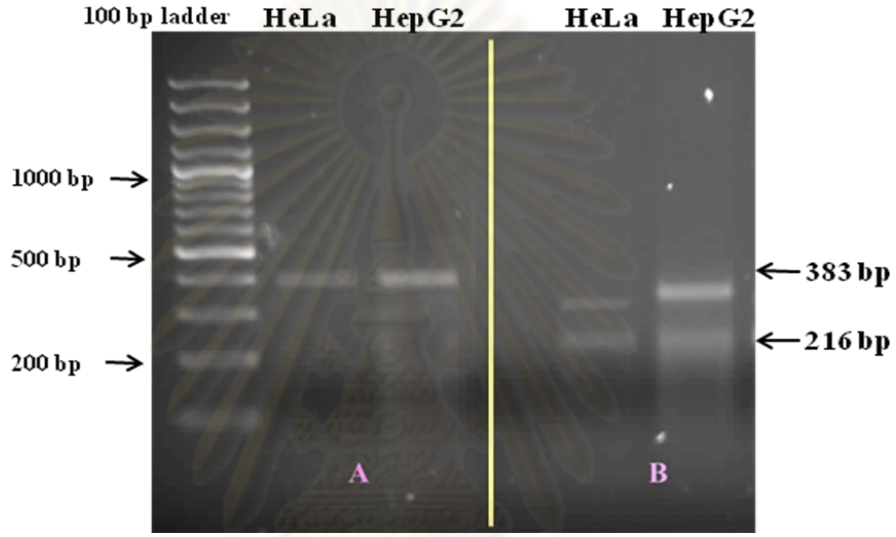

Figure 28 Comparison of RAGE gene amplification by (A) F1 and R1 primers and (B) F1 and R2 primer at 65 °C annealing temperature respectively.

4.1.4) β-actin primers (product size 656 bp).

β-actin gene was tested for optimized annealing temperature from 58 °C – 61 °C. The result from figure 29 showed that the temperature at 58 °C is the best.

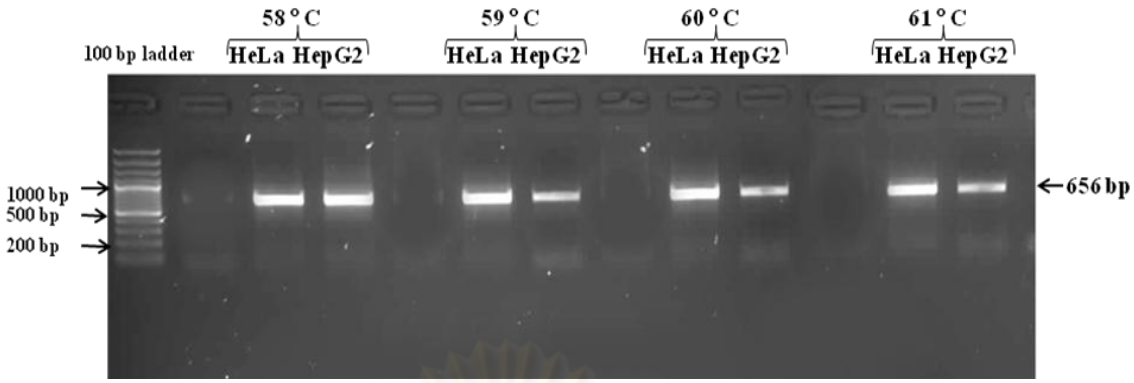

Figure 29 β-actin gene amplification of HeLa cell line and HepG2 cell line at 58 °C, 59 °C, 60 °C and 61 °C respectively**.**

4.2) Condition for electrochemical biosensor

4.2.1) Appropriate RNA concentration from HeLa cell line and HepG2 cell line for electrochemical biosensor

Total RNA of HeLa and HepG2 cell lines were extracted by commercial kit and Tri-RNA protocol. Extracted RNA was diluted to 1200 ng and 1600 ng and used for amplification of RAGE gene **(figure 30).**

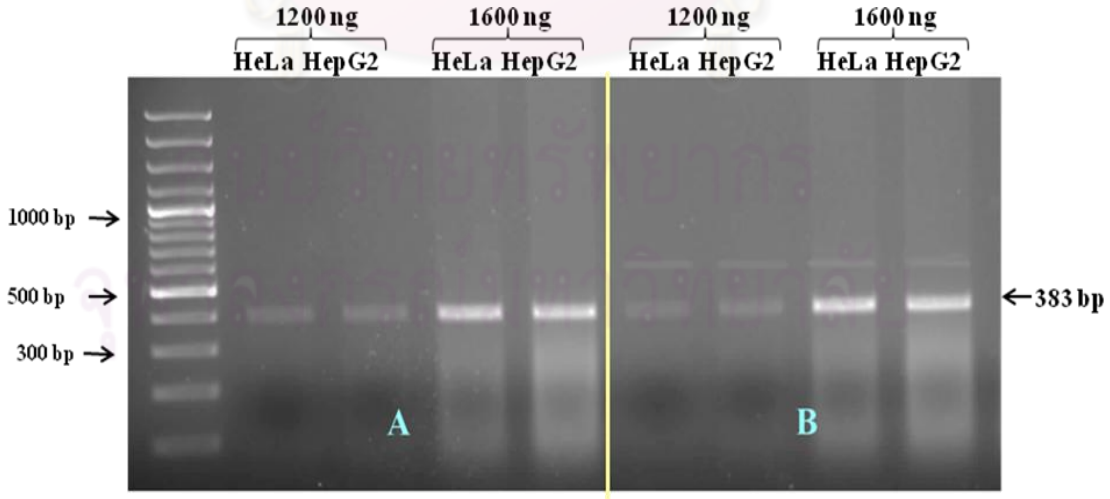

Figure 30 RAGE gene amplification for1200 ng and 1600 ng RNA of HeLa cell line and HepG2 cell lines respectively by using (A) commercial kit and (B) Tri-RNA

The result showed that the commercial kit was better than Tri-RNA because it gave one specific band. The proper concentration is 1200 ng RNA because there are smear band less than 1600 ng and 1200 ng RNA had one specific band whereas 1600 ng RNA appeared to have non specific band. Then, 300 ng RNA and 1200 ng RNA was amplified for RAGE gene (**figure 31)**. The result showed that 300 ng was invisible on agarose gel separation, but 1200 ng was visible. So, this two concentrations were use to compare sensitivity between conventional gel electrophoresis and electrochemical biosensor. In addition, the PCR condition for RAGE gene and β-actin gene were as mentioned above.

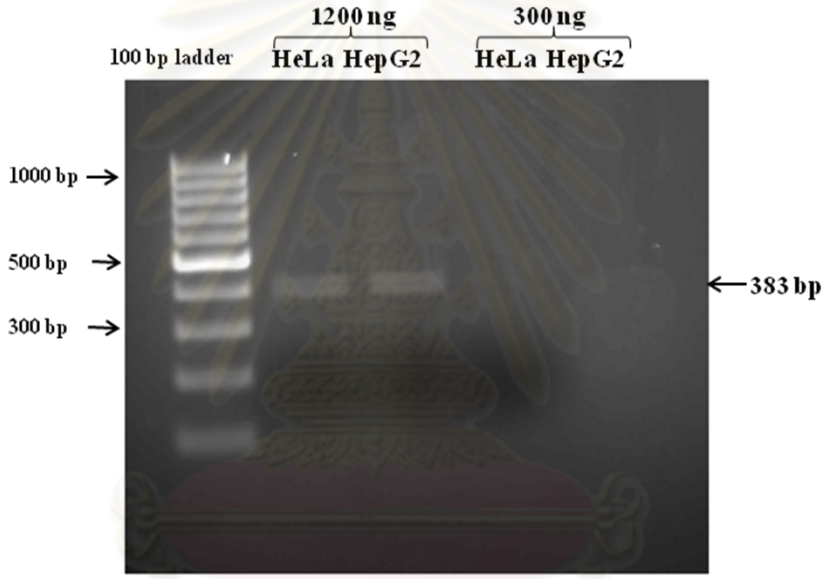

Figure 31 Separation of RAGE gene amplification for 1200 ng and 300 ng RNA of HeLa and HepG2 cell lines upon agarose gel electrophoresis.

4.3) Optimization of conditions for electrochemical biosensor detection

4.3.1) Appropriate phosphate-buffered saline (PBS) concentration and pH

PCR product of RAGE gene was mixed with 25, 50, 100 and 200 mM PBS at pH 6.4, 7.4 and 7.8 to reach the final Hoechst 33258 concentration of 20 μM. The mixture was loaded on EP-N chip, and anodic current (microampere) was measured by linear sweep voltammetry (LSV). The anodic current peaks were plotted in line chart as shown in figure 32.

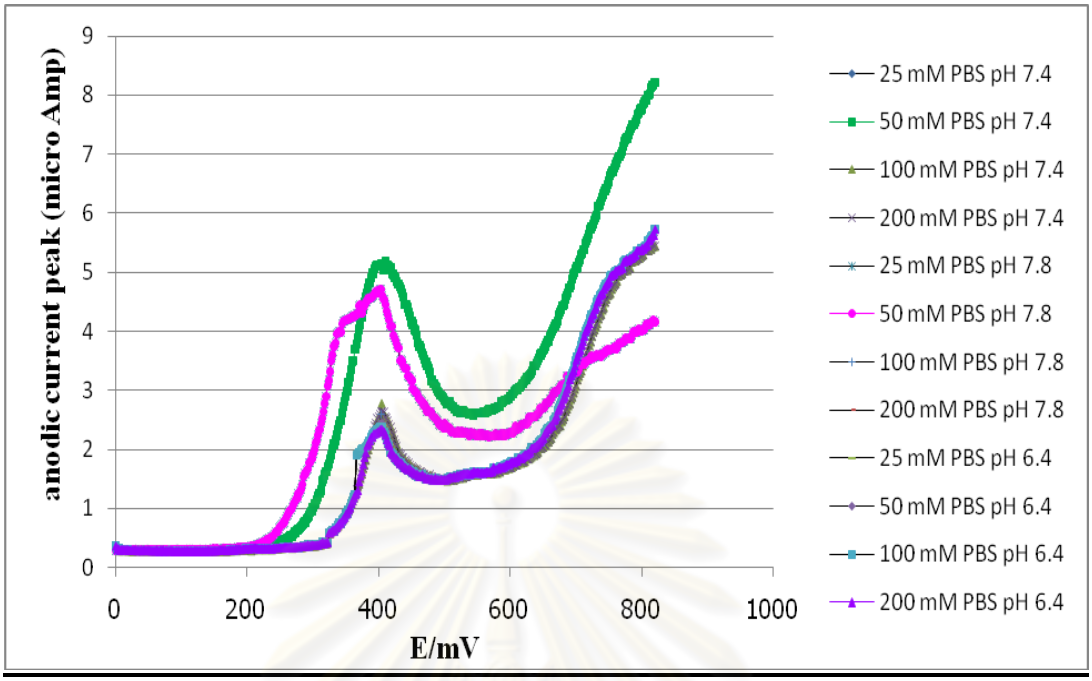

Figure 32 Anodic current peak of RAGE positive PCR products when various PBS conditions were used.

The results showed that PBS at 50 mM at pH 7.4 gave the highest anodic current peak. RAGE gene negative control PCR product (0 copy) were also tested in the same manner and the results were shown in figure 33. Then, the anodic current peak of positive and negative were compared as shown in figure 34

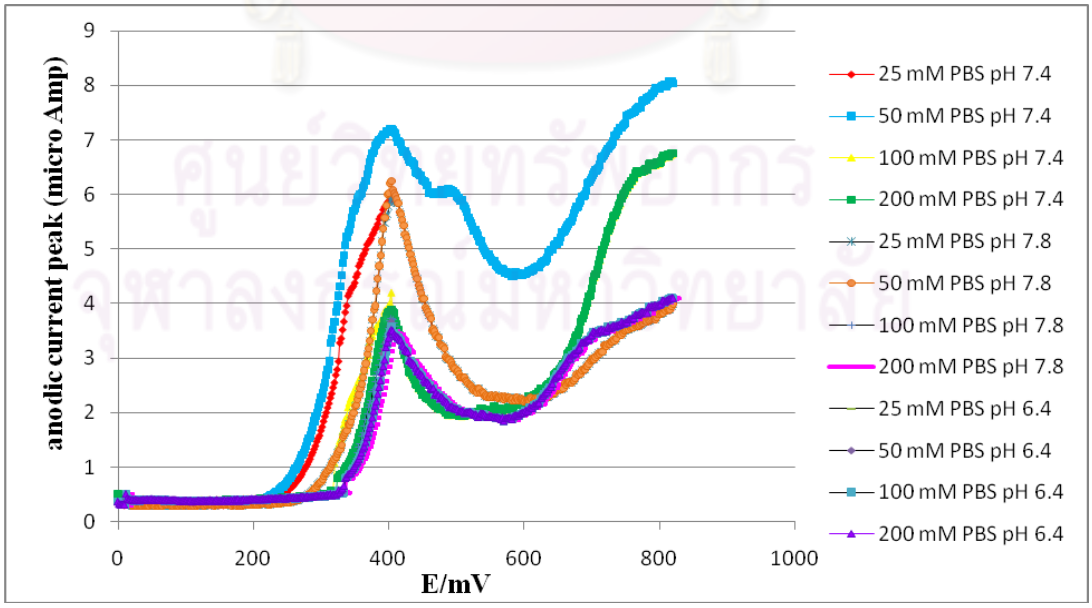

Figure 33 Anodic current peak of RAGE negative PCR products when various PBS conditions were used.

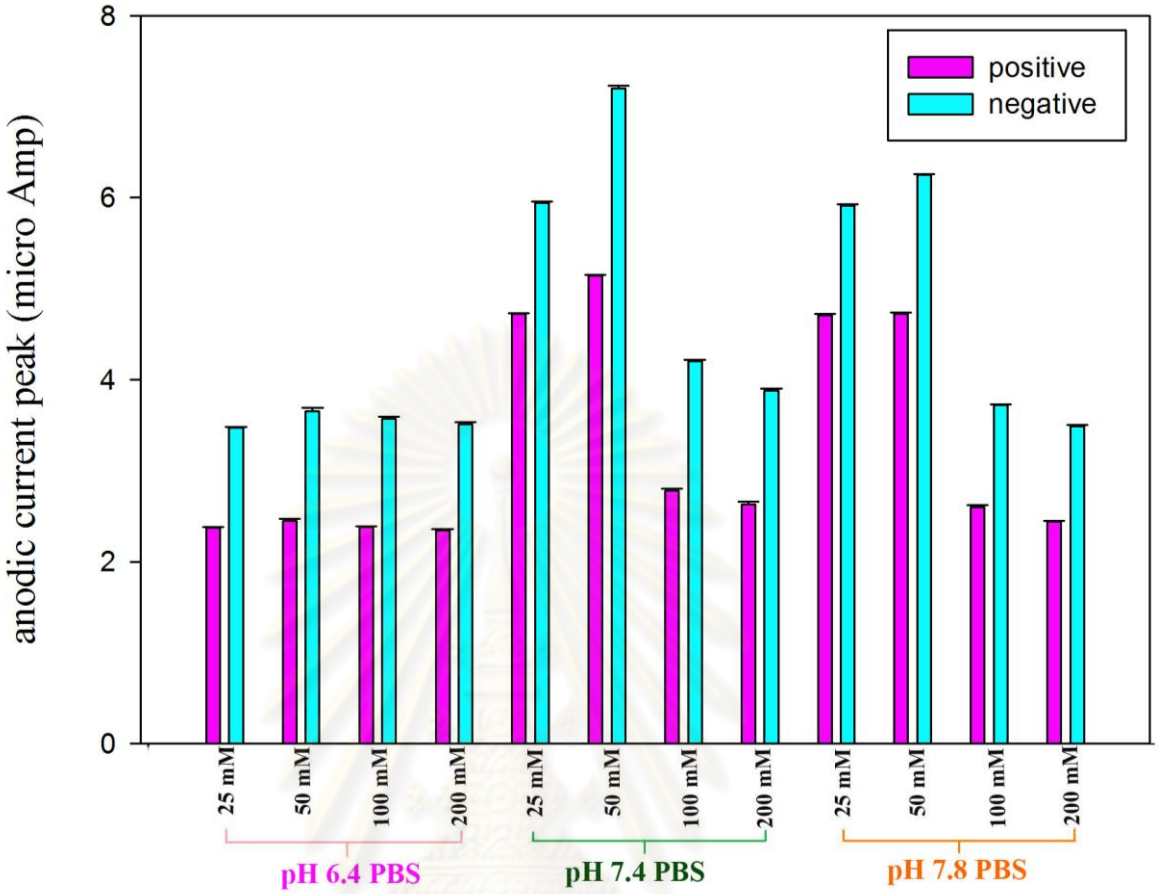

Figure 34 Comparison of anodic current peak from EP-N chip of RAGE positive and negative PCR products when various PBS conditions were used**.**

For electrochemical detection using Hoechst 33258, the greater the difference between positive anodic current peak and negative anodic current peak, the better the sensitivity of detection as shown in table 1.

Table 1 Anodic current peaks and the difference between positive and negative PCR products of RAGE from EP-N chip

PBS conditions	Anodic current peak (microampere)		
	Positive control	Negative control	Difference
pH 6.4			
25 mM	2.37	3.47	1.1
50 mM	2.45	3.65	1.2
100 mM	2.38	3.57	1.19
200 mM	2.34	3.51	1.17
pH 7.4			
25 mM	4.72	5.94	1.22
50 mM	5.14	7.2	2.06
100 mM	2.78	4.2	1.42
200 mM	2.63	3.88	1.25
pH 7.8			
25 mM	4.71	5.91	1.2
50 mM	4.72	6.25	1.53
100 mM	2.6	3.72	1.12
200 mM	2.44	3.49	1.05

The results from both positive and negative controls showed that PBS at 50 mM, pH 7.4 provided the highest anodic currents at 5.14 and 7.20 microampere respectively and gave the highest difference.

Comparison EP-N chip with SP-P chip

Similar to EP-N chip, the same condition of PBS were mixed with positive and negative RAGE PCR and anodic current peak were measured and plotted in bar chart as shown in figure 35.

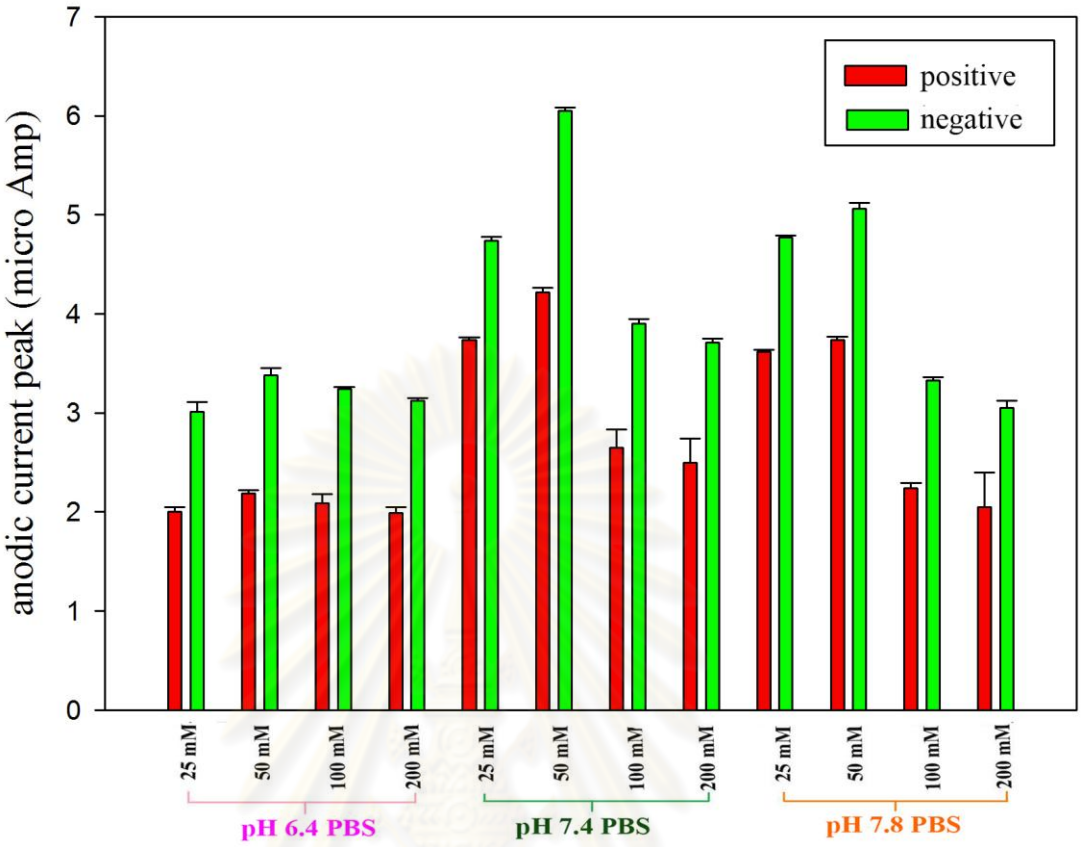

Figure 35 Comparison of anodic current peak from SP-P chip of RAGE positive and negative PCR products when various PBS conditions were used.

The difference from the positive and negative anodic current peak were shown in table 2.

Table 2 Anodic current peaks and the difference between positive and negative PCR products of RAGE from SP-P chip

PBS conditions	Anodic current peak (microampere)		
	Positive control	Negative control	Difference
pH 6.4			
25 mM	2.00	3.01	1.01
50 mM	2.19	3.38	1.19
100 mM	2.09	3.24	1.15
200 mM	1.99	3.12	1.13
pH 7.4			
25 mM	3.74	4.74	1.00
50 mM	4.22	6.05	1.83
100 mM	2.65	3.90	1.25
200 mM	2.50	3.71	1.21

pH 7.8			
25 mM	3.62	4.77	1.15
50 mM	3.74	5.06	1.32
100 mM	2.24	3.33	1.09
200 mM	2.05	3.05	1.00

From the result, PBS at 50 mM, pH 7.4 provided the highest difference like EP-N chip but SP-P chip gave the anodic current peak lower than EP-N and had the standard variation higher than EP-N. So, EP-N chip was used in this method with Hoechst 33258 dissolved in 50 mM PBS, pH 7.4.

4.3.2) Appropriate concentration of Hoechst 33258

In order to test whether increased Hoechst 33258 concentration can increase sensitivity of detection, 20 µM or 50 µM Hoechst 33258 were mixed with 50 mM PBS pH 7.4 and then mixed with positive and negative PCR products.

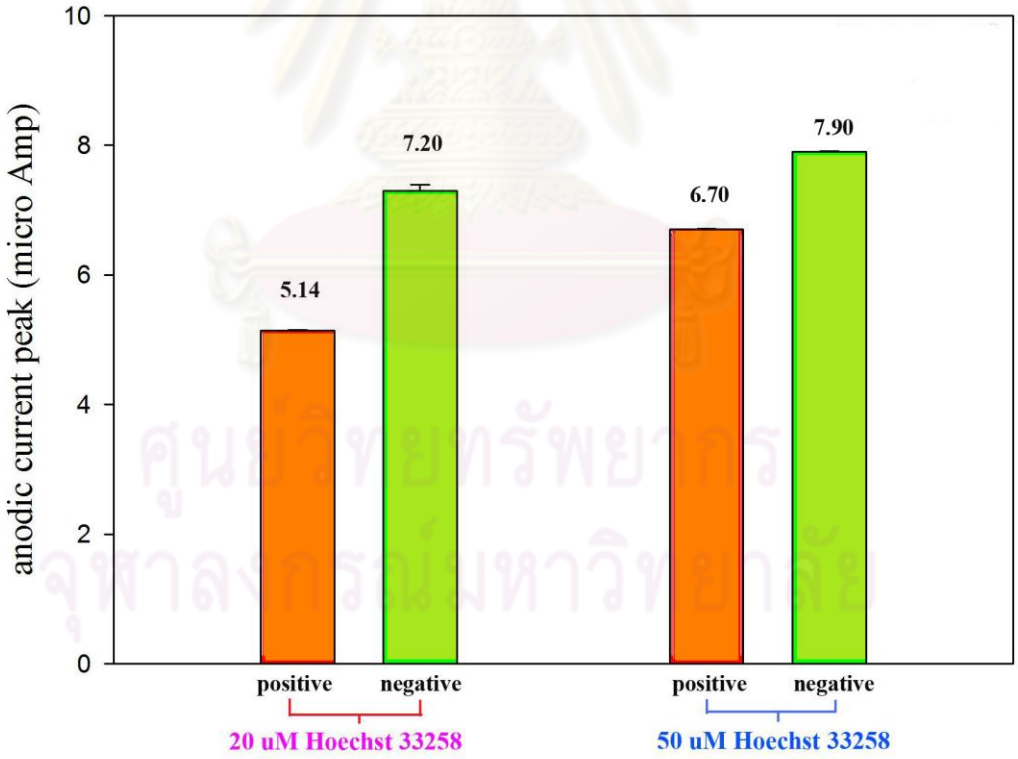

Figure 36 Anodic current peak from RAGE positive and negative PCR mixed with 20 µM and 50 µM Hoechst 33258.

According to **figure 36**, the anodic current peak of 20 µM Hoechst 33258 when mixed with positive and negative PCR product were 5.14 and 7.2 microampere respectively and difference between the two anodic current peaks was 2.06 microampere while the anodic current peak of 50 µM Hoechst 33258 when mixed with positive and negative PCR product were 6.70 and 7.90 microampere respectively and the difference was 1.2 microampere. Since 20 µM Hoechst 33258 gave greater difference, this concentration was used for detection of β-actin and RAGE PCR products.

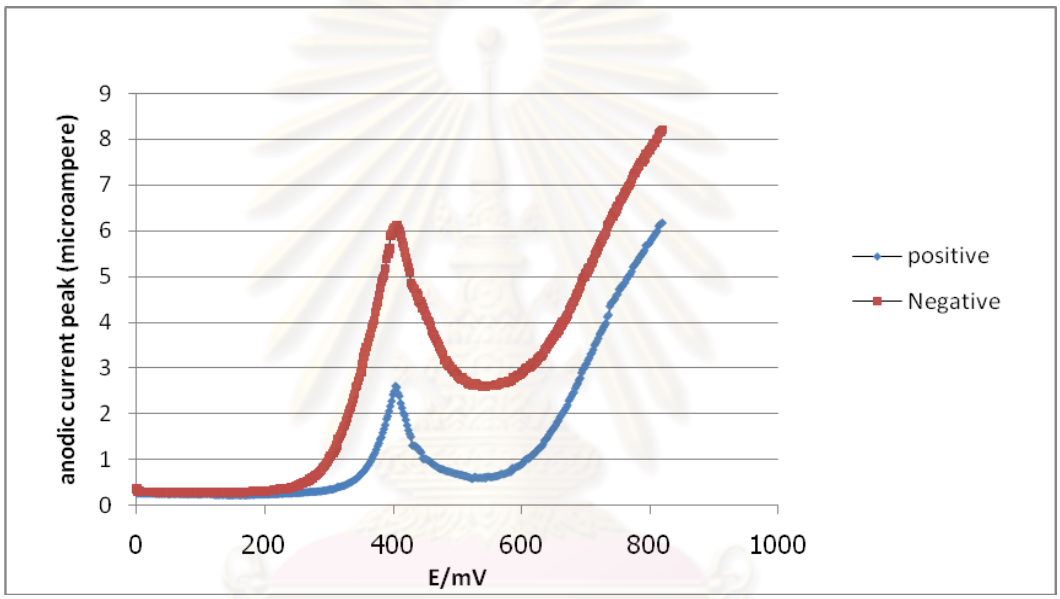

Figure 37 Line chart for anodic current peak from β-actin positive and negative PCR product when mixed with 20 µM Hoechst 33258.

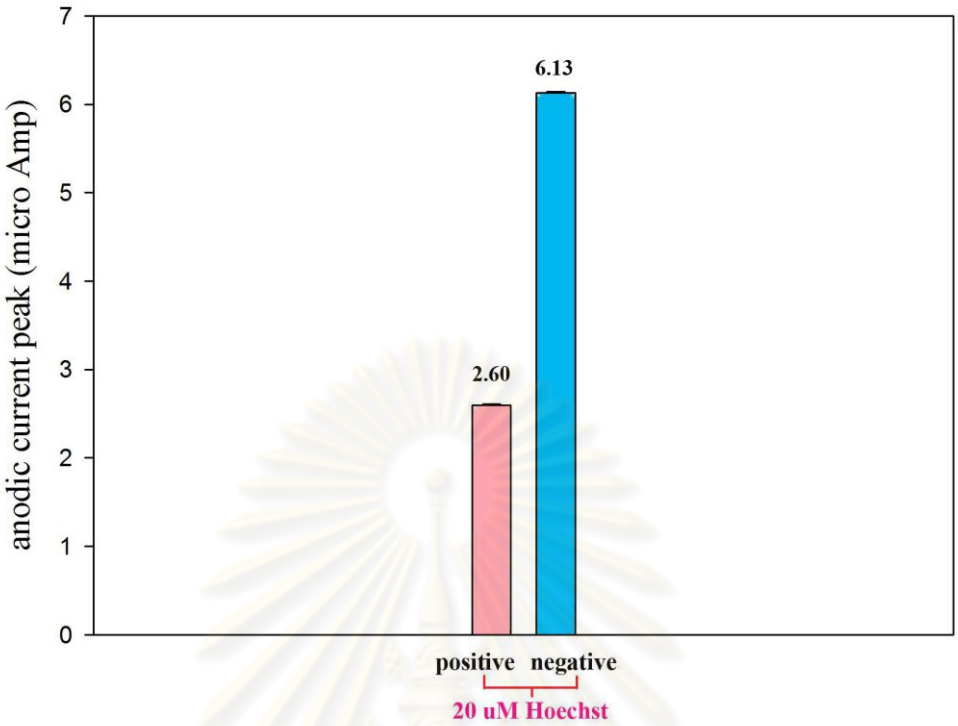

Figure 38 Difference in anodic current peak from β-actin positive and negative PCR product when mixed with 20 µM Hoechst 33258.

From figures 37 and **38**, the anodic current peaks of β-actin positive and negative PCR product were 2.6 and 6.13 microampere respectively and the difference between the two current peaks was 3.53 microampere.

4.4) Precision of electrochemical biosensor method

Within day precision

β-actin DNA standards at low level (10^4 copies) and high level (10^9 copies) were measured repeatedly for 10 times and coefficient of variation (% CV) was 4.68 % and 1.88% for the high and low levels respectively.

RAGE DNA standards at low level (10 copies) and high level (10^9 copies) were measured repeatedly for 10 times and coefficient of variation (% CV) was 2.25 % and 3.74 % for the high and low levels respectively.

Between day precision

β-actin DNA standards at low level (10^4 copies) and high level (10^9 copies) were measured repeatedly for 30 times in 10 days and coefficient of variation (% CV) was 4.94 % and 2.02 % for the high and low levels respectively.

RAGE DNA standards at low level (10 copies) and high level (10^9 copies) were measured repeatedly for 30 times in 10 days and coefficient of variation (% CV) was 2.38 % and 3.89 % for the high and low levels respectively.

4.5) Standard curves of β-actin and RAGE genes

Standard curves of β-actin gene were created for both agarose gel electrophoresis method and electrochemical biosensor method. The results in figure 39 showed that the lowest detectable concentration of β-actin gene was10^4 copies and figure 40 demonstrated bands of β-actin from HeLa and HepG2 when DNA concentrations of 75 ng (A) and 300 ng (B) were used. The lowest concentration of β-actin DNA which can be detected by agarose gel electrophoresis was10^4 copies

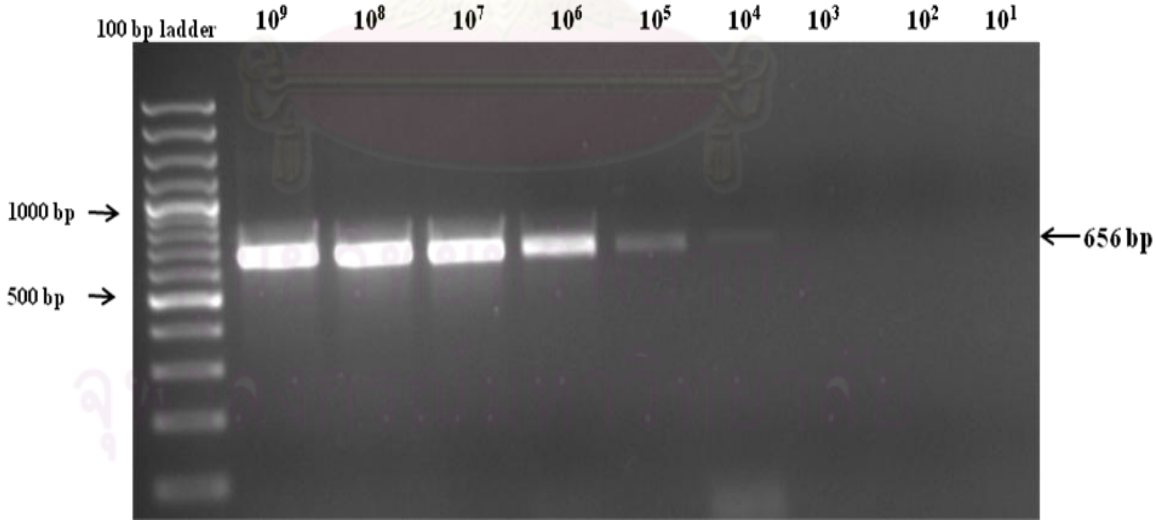

Figure 39 The lowest concentration of β-actin DNA which can be detected by agarose gel electrophoresis was10^4 copies.

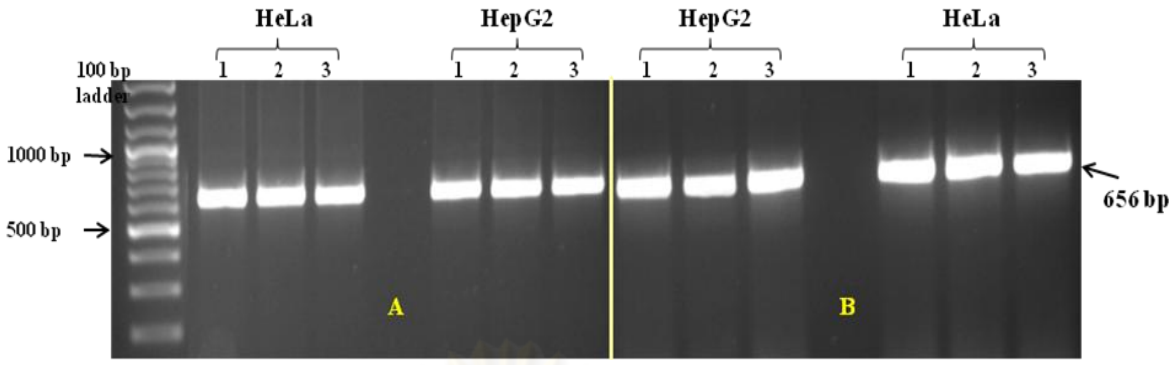

Figure 40 Bands of β-actin from HeLa and HepG2 when different amount of PCR products were loaded for agarose gel electrophoresis, A) 75 ng, B) 300 ng. The experiments were done in triplicate.

Log copy number of β-actin was plot versus band density from agarose gel electrophoresis and standard curve was created (linear equation: y = 566851.073 x + 817029.456; R^2 = 0.9646) as shown in figure 41 A. Standard curve of RAGE was shown in figure 41 B (y = 519408.070 X + 1161581.659; R^2 = 0.9967).

A

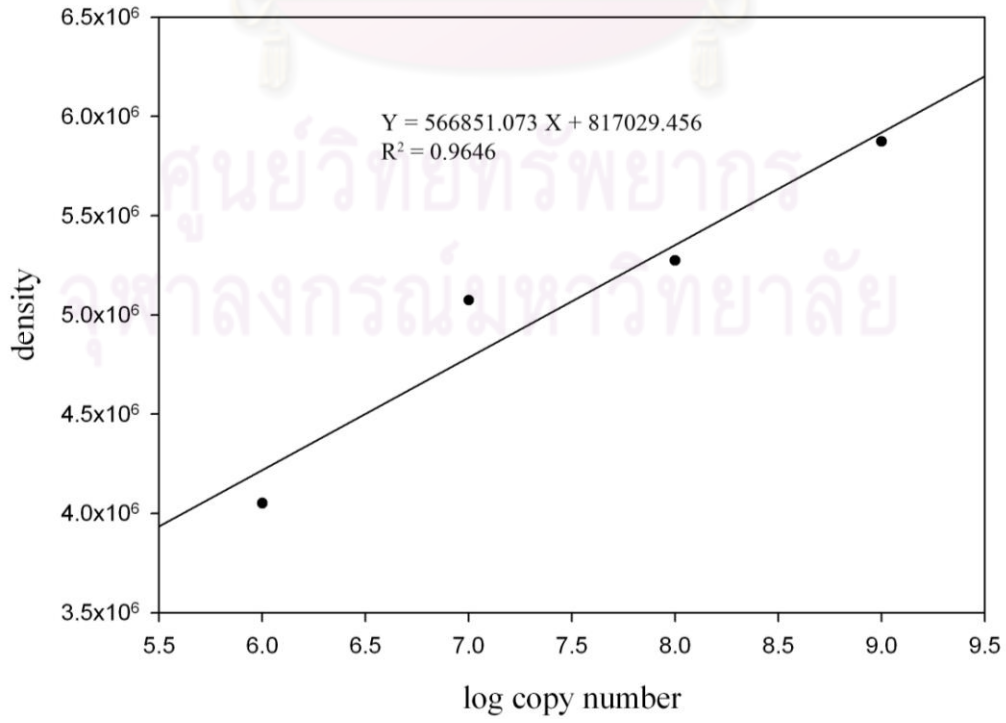

B

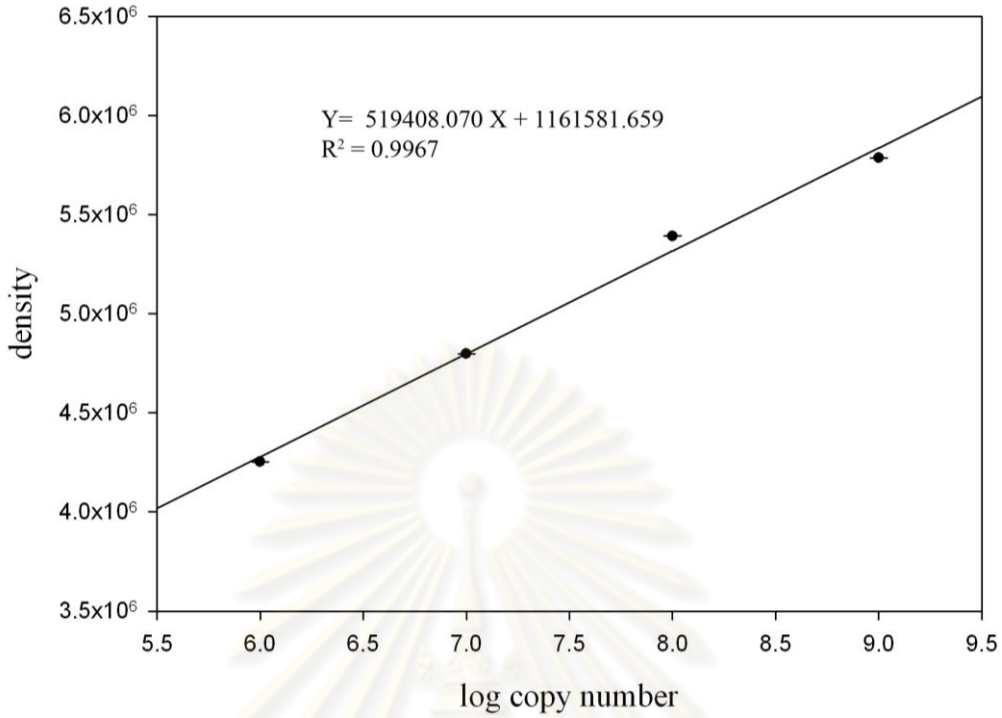

Figure 41 Standard curve from a plot between log copy number and band density from electrophoretogram of the conventional electrophoresis method for (A) β-actin gene (B) RAGE gene.

For electrochemical biosensor detection, the current was dependent on free Hoechst 33258 molecules in the mixture, thus the current peak was inversely proportional to DNA concentration. Standard curve of β-actin gene was plot between log copy number and anodic current peak ($y = 5.8249 – 0.3523\ x$; $R^2 = 0.9783$) as shown in figure 42 A. Samples were measured and copy numbers of β-actin were determined from standard curve. Likewise, standard curve of RAGE gene was created from regression equation ($y = 7.1590 – 0.2270\ x$; $R^2 = 0.9937$) as shown in figure 42 B.

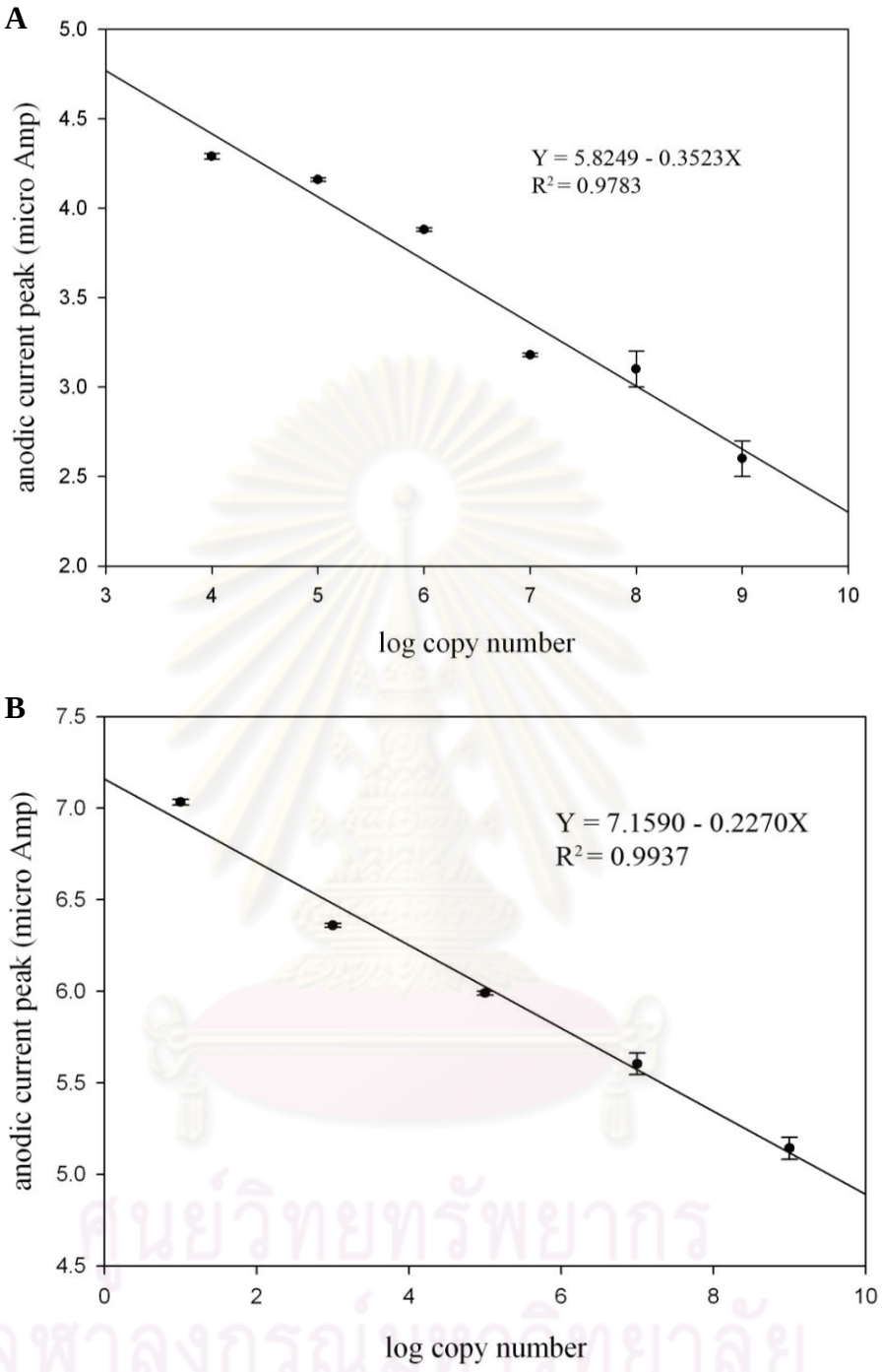

Figure 42 Standard curve of electrochemical biosensor method for semi-quantitative detection of (A) β-actin gene (B) RAGE gene.

4.6) Comparison of gene expression between two methods

The copy numbers of β-actin gene were determined from electrochemical biosensor and agarose gel electrophoresis. The concentration of β-actin gene (copy numbers) were compared between the two techniques as shown as table 3.

Table 3 Comparison of β-actin gene concentration (copies numbers) obtained from electrochemical biosensor and conventional agarose gel electrophoresis.

Measurement	75 ng/ 5µl of cDNA					
	Hela cell lines			HepG2 cell lines		
	No.1	No.2	No.3	No.1	No.2	No.3
Anodic peak (µA) B-actin gene	3.52	3.51	3.52	3.54	3.54	3.55
Copy number of B-actin gene (copies)						
electrochemical biosensor	3,467,369	3,715,352	3,467,369	3,090,295	3,090,295	2,884,032
conventional PCR	3,467,369	3,548,134	3,467,369	3,019,952	3,019,952	3,019,952
Measurement	**300 ng/ 5µl of cDNA**					
	Hela cell lines			**HepG2 cell lines**		
	No.1	**No.2**	**No.3**	**No.1**	**No.2**	**No.3**
Anodic peak (µA) B-actin gene	2.74	2.74	2.75	2.76	2.76	2.77
Copy number of B-actin gene (copies)						
electrochemical biosensor	575,439,937	575,439,937	537,031,796	501,187,234	501,187,234	467,735,141
conventional PCR	562,341,325	562,341,325	549,540,870	489,778,819	501,187,234	489,778,819

From table 2, measurements from the two methods were compared and analyzed by Passing–Bablok regression as shown in figure 43.

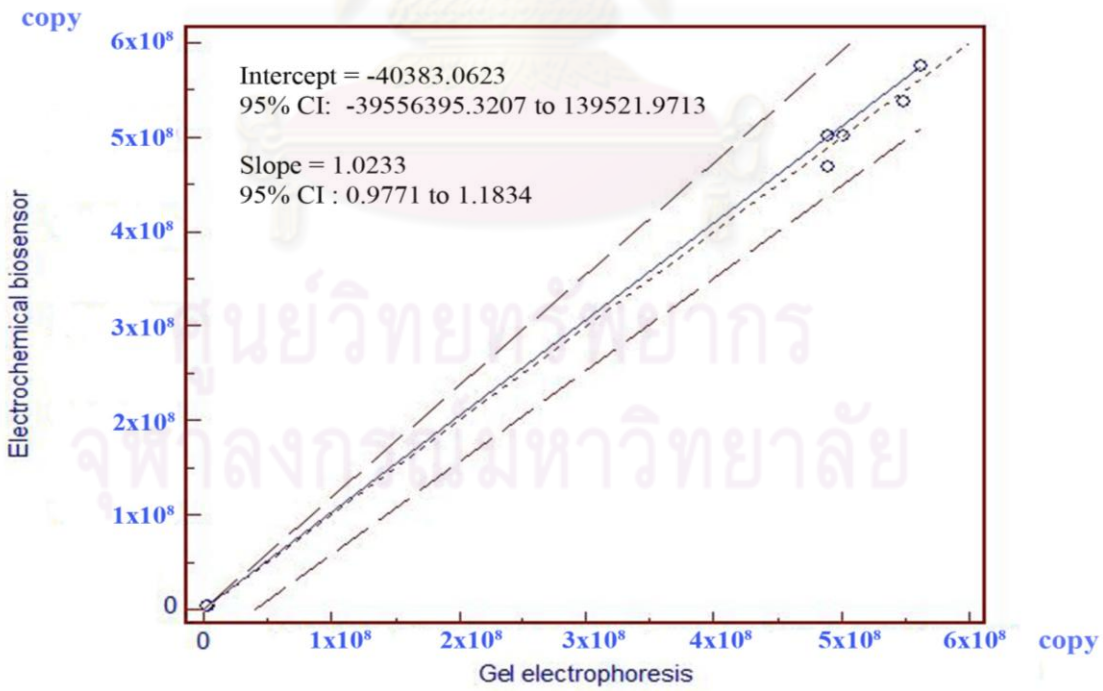

Figure 43 Comparison between the electrochemical biosensor and the conventional agarose gel electrophoressis for β-actin semiquantitation using Passing–Bablok regression analysis.

The equation from Passing–Bablok regression was y = - 40383.0623 + 1.0233 x and the slope of 1.0233 fit with 95% confidence limit of 0.9771- 1.1834 as shown in table 4. This result suggested that the electrochemical biosensor correlated well with the conventional agarose gel electrophoresis.

Table 4 Passing–Bablok regression analysis showed good correlation between gel electrophoresis and electrochemical biosensor methods**.**

Passing and Bablok regression

Variable X	Gel_electrophoresis Gel electrophoresis
Variable Y	Electrochemical_biosensor Electrochemical biosensor
Sample size	12

	Variable X	Variable Y
Lowest value	3019952.0000	2884032.0000
Highest value	562341325.0000	575439937.0000
Arithmetic mean	264542593.3333	264811332.5833
Median	246663476.5000	235725246.5000
Standard deviation	273973541.6295	274753377.9307
Standard error of the mean	79089349.0053	79314468.3545

Regression Equation

y = -40383.0623 + 1.0233 x	
Intercept A	-40383.0623
95% CI	-39556395.3207 to 139521.9713
Slope B	1.0233
95% CI	0.9771 to 1.1834
Cusum test for linearity	No significant deviation from linearity (P>0.10)

4.7) Application for detection of gene of interest

Electrochemical biosensor aggregation with Hoechst 33258 was applied for detection of RAGE gene from HeLa and HepG2, using cDNA from the same tube of β-actin gene amplification. The copy number of RAGE gene was interpolated from standard curve and RAGE gene expression was calculated in relative to β-actin gene, the results were shown in table 5.

Table 5 Determination of RAGE gene concentrations in HeLa and HEPG2 cell lines by estimation of copy number of RAGE relative to β-actin (RAGE/ β-actin).

Measurement	75 ng/ 5µl of cDNA					
	Hela cell lines			HepG2 cell lines		
	No.1	No.2	No.3	No.1	No.2	No.3
Anodic peak (µA)						
RAGE gene	6.36	6.36	6.37	6.44	6.44	6.45
B-actin gene	3.52	3.51	3.52	3.54	3.54	3.55
Copy number (copies)						
RAGE gene	3,311	3,311	3,020	1,479	1,479	1,318
B-actin gene	3,467,369	3,715,352	3,467,369	3,090,295	3,090,295	2,884,032
Estimated RAGE gene concentration	**0.0009549**	**0.0008912**	**0.0008710**	**0.0004786**	**0.0004786**	**0.0004570**
Measurement	**300 ng/ 5µl of cDNA**					
	Hela cell lines			**HepG2 cell lines**		
	No.1	**No.2**	**No.3**	**No.1**	**No.2**	**No.3**
Anodic peak (µA)						
RAGE gene	5.86	5.86	5.87	5.94	5.95	5.96
B-actin gene	3.52	3.51	3.52	3.54	3.54	3.55
Copy number (copies)						
RAGE gene	524,807	524,807	478,630	234,423	257,040	190,546
B-actin gene	575,439,937	575,439,937	537,031,796	501,187,234	501,187,234	467,735,141
Estimated RAGE gene concentration	**0.0009120**	**0.0009120**	**0.0008913**	**0.0004677**	**0.0005129**	**0.0004074**

When different concentrations of cDNA were used, the relative values of estimated RAGE cDNA concentration from HeLa and HepG2 were analyzed by paired t-test shown in table 6 according to the following hypothesis.

H_0: no difference between two values

H_1: difference between two values

$\alpha = 0.05$

If significant (2- tailed) value > α means accept H_0

If significant (2- tailed) value < α means reject H_0

Paired Samples Statistics

		Mean	N	Std. Deviation	Std. Error Mean
Pair 1	ratio75	0.00068855	6	0.000239613	0.000097821394
	ratio300	0.000683883	6	0.000244749	0.000099918245

Paired Samples Correlations

		N	Correlation	Sig.
Pair 1	ratio75 & ratio300	6	0.989	0

Paired Samples Test

		Paired Differences					t	df	Sig. (2-tailed)
		Mean	Std. Deviation	Std. Error Mean	95% Confidence Interval of the Difference				
					Lower	Upper			
Pair 1	ratio75 - ratio300	0.000004666667	0.000035524452	0.000014502797	-0.000032613959	0.000041947292	0.322	5.0	0.761

Table 6 Paired t-test for analysis of the difference of means of relative value of RAGE cDNA between HeLa and HepG2

The result from table 6 showed no statistically significant difference between RAGE gene copy numbers when 75 ng or 300 ng of DNA were used (p= 0.761) or accept H_0 because of 0.761 > 0.05. The average RAGE gene expression of HeLa and HEPG2 were 0.0009051 and 0.0004670 respectively. So, HeLa cells expressed twice more RAGE gene than HepG2 cells.

When the same samples of RAGE cDNA at various concentrations were measured semi-quantitatively, the results demonstrated that the electrochemical biosensor was more sensitive than the conventional electrophoresis method (figures 41). The lowest concentrations of RAGE gene band which can be visualized was 10^4 copies (figure 44) but the lowest detection in linearity range of electrophoresis method was 10^6 copies (figure 41 B) compared to10 copies for the biosensor method (figure 42 B). RAGE gene was expressed more in HeLa cells than in HepG2 (figure 45).

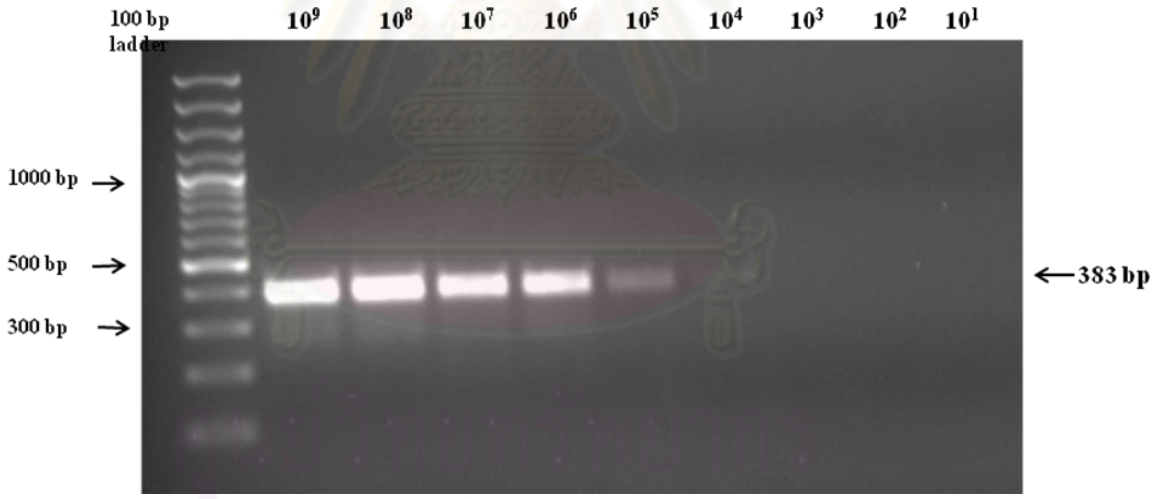

Figure 44 The lowest concentration of RAGE DNA which can be detected by agarose gel electrophoresis was10^4 copies.

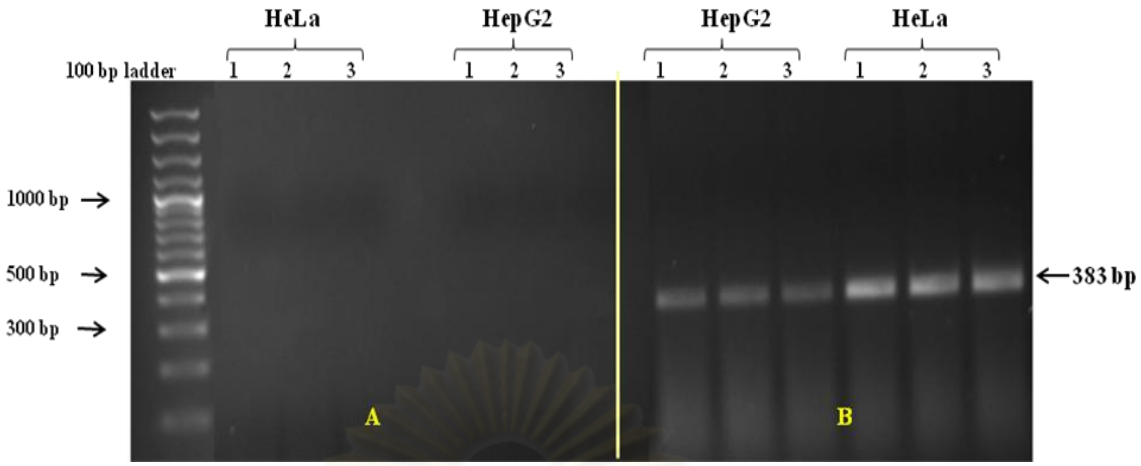

Figure 45 RAGE DNA from HeLa and HepG2 could be detected only at application of 300 ng (B), not at 75 ng (A), the experiments were done in triplicate**.**

Chapter V

Discussion and Conclusion

5.1) Discussion

Electrochemical biosensor using electrochemical indicator for direct or indirect detection is faster than guanine oxidation because the signal that is generated by the former is higher and sharper than the latter signal **(25)**. There are many types of indicators for this technique but using intercalator as the indicator especially Hoechst 33258 is more useful than other types **(1)**. Since Hoechst 33258 binds to minor groove of double strand DNA at A-T rich region better other region **(49, 51, 52)** and bind specifically to dsDNA, it is used for detection the hybridization between specific target and immobilizing probes in the reaction **(55)**.

Electrochemical biosensor detection depends on the immobilizing probe on the electrode. Thus, this technique inducing with Hoechst 33258 was applied for detection of DNA. This technique is fast and easy to perform because it shortcuts the probe immobilizing step. There was a study that used electrochemical biosensor for detecting gene expression in plant tissues but they used enzyme-linked DNA hybridization assay **(121)**. In this study, the precision of electrochemical biosensor is less than 5% that means good method performance **(122)**. The electrochemical biosensor aggregation with Hoechst 33258 was applied for detection of gene expression of the highly expressed gene, β-actin, and compared with conventional agarose gel electrophoresis method. The technique was then applied to detect the gene of interest which was lowly expressed, RAGE gene, from HeLa and HepG2 cell lines. The result from this study demonstrated that, the electrochemical biosensor is faster than conventional electrophoresis method as shown in table7 because it can reduce time for electrophoresis and ethidium bromide staining, overall time for detection gene by biosensor technique is thirty minutes while agarose gel electrophoresis needs more than one hour. Particularly, electrochemical detection was more sensitive than the electrophoresis method because it can detect RAGE gene at the lowest level of 10 copies whereas the gel electrophoresis method can detect semi-quantitative only at concentration over 10^6 copies.

Table 7 Comparison of two techniques

	Conventional method	Electrochemical biosensor
Sensitivity	can be visualized at 10^4 copies and can detect semi-quantitatively at 10^6 copies	can detect semi-quantitatively at 10 copies
Time per test	more than hour	thirty minutes
Cost per test (10 tests)	130 baht	114 baht

This technique is sensitive and easy to use because it does not require specific skill and reduces cost and time; however it requires one specific band of PCR amplification product, because the non specific band may interfere with the electrochemical signal. Therefore, specific primers are needed for DNA amplification. For RAGE gene, design of specific primers was rather difficult because it has many variants **(60)**, thus limits the design for appropriate length of product and the selection for A-T rich region. In this study, PCR was performed with 30 cycles which was effective to avoid PCR saturation. For Hoechst 333258, beside A-T region, pH of buffer can affect the efficiency of Hoechst 33258 **(123)**. Normally, the working pH for Hoechst 33258 is pH 7.4 which is physiological condition **(124, 125)** and there is a study using Hoechst 33258 for staining plant cell protoplasts. They found that the optimum pH is pH 7.5 **(126).** So, pH 7.4 - 7.5 is suitable for Hoechst 33258 dye. For detection process, the different DEP chips between EP-N and SP-P model were used in order to compare the anodic current peak. The result shows that EP-N chip is better than SP-P because the mixture on SP-P with square working electrode can flow out the working electrode that causes low anodic current peak and high standard deviation (S.D.) and air bubble on electrode must be avoided because it can cause error signal. In addition culture condition may cause changing RAGE expression because there are studies about RAGE expression in podocytes in the glomerulus which found that interaction of cells with plastic and coated dishes and/or their exposure to high levels of growth factors in fetal serum can upregulate RAGE antigen selectively in vitro

where as in vivo mesangial or renal tubular cells normally do not appear to express RAGE, even in disease states **(82, 127-129)**. To increase efficiency of electrochemical biosensor using Hoechst 33258, electrode could be modified from carbon to gold **(56)** but the cost will increase.

5.2) Conclusion

The electrochemical method can be used for semi-quantitative detection of gene expression and can be adapted for the rapid screening method of many genes including the lowly expressed genes of interest.

References

(1) Hashimoto, K., Ito, K., and Ishimori, Y. (1994). Novel DNA sensor for electrochemical gene detection. Anal Chim Acta 286: 219-224.

(2) Nagaev, I., and Smith, U. (2001). Insulin resistance and type 2 diabetes are not related to resistin expression in human fat cells or skeletal muscle. Biochem Biophys Res Commun 285 (2): 561-564.

(3) Bernard, PS., and Wittwer, CT. (2002). Real-time PCR technology for cancer diagnostics. Clin Chem 48 (8): 1178-1185.

(4) Wang, J. (2000). Survey and summary from DNA biosensor to gene chips. Nucleic Acids Res 28 (16): 3011-3016.

(5) Scheller, F., Wollenberger, U., Warsinke, A., and Lisdat, F. (2001). Research and development in biosensors. Curr Opin Biotech 12: 35-40.

(6) Okamoto, A., Kamei, T., Tanaka, K., and Saito, I. (2004). Electrochemical behavior of gold electrodes modified with photosensitizer-tethered DNA. Nucleic Acids Symp Ser (Oxf) (48): 71-72.

(7) Cagnin, S., Caraballo, M., and Guiducci, C. (2009). Overview of Electrochemical DNA Biosensors: New Approaches to Detect the Expression of Life. Sensors 9: 3122-4318.

(8) Wang, S., Peng, T., and Yang, CF. (2003). Investigation on the interaction of DNA and electroactive ligands using a rapid electrochemical method. J Biochem Biophys Methods 55 (3): 191-204.

(9) Kobayashi, M., Kusakawa, T., Saito, M., and Kaji, S. (2004). Electrochemical DNA quantification based on aggregation induced by Hoechst 33258. Electrochem Commun 6 (4): 337–343.

(10) Chaumpluk, P., Chikae, M., Takamura, Y., and Tamiya, E. (2006). Novel electrochemical identification and semi quantification of bovine constituents in feedstuffs. Science and Technology of Advanced Materials 7 (3): 263-269.

(11) Schmidt, AM., Yan, SD., Wautier, JL., and Stern, D. (1999). Activation of receptor for advanced glycation end products: a mechanism for chronic vascular dysfunction in diabetic vasculopathy and atherosclerosis. Circ Res 84 (5): 489-497.

(12) Schmidt, A.M., and Stern, D. (2000). Atherosclerosis and diabetes: the RAGE connection. Curr Atheroscler Rep 2 (5): 430-436.

(13) Hiwatashi, K., et al. (2008). A novel function of the receptor for advanced glycation end-products (RAGE) in association with tumorigenesis and tumor differentiation of HCC. Ann Surg Oncol 15 (3): 923-933.

(14) Daroux, M., et al. (2010). Advanced glycation end-products: implications for diabetic and non-diabetic nephropathies. Diabetes Metab 36 (1): 1-10.

(15) Zhang, FL., Gao, HQ., and Shen, L. (2007). Inhibitory effect of GSPE on RAGE expression induced by advanced glycation end products in endothelial cells. J Cardiovasc Pharmacol 50 (4): 434-440.

(16) D'Orazio, P. (2003). Review Biosensors in clinical chemistry. Clin Chim Acta 334 (1-2): 41-69.

(17) Pohanka, M., and Skladal, P. (2008). Electrochemical biosensors-principles and applications. J Appl Biomed 6 (2): 57-64.

(18) Mascini, M., Palchetti, I., and Marrazza, G. (2001). DNA electrochemical biosensors. Fresen J Anal Chem 369: 15-22.

(19) Mohanty, SP., and Kougianos, E. (2006). Biosensors: a tutorial review. Potentials, IEEE 25 (2): 35-40.

(20) Palek, E., and Fojta, M. (2001). Peer Reviewed: Detecting DNA Hybridization and Damage. Anal Chem 73 (3): 74-83.

(21) Drummond, T., Hill, MG., and Barton, JK. (2003). Electrochemical DNA sensors review. Nat Biotechnol 21 (10): 1192-1199.

(22) Cosnier, S., and Mailley, P. (2008). Recent advances in DNA sensors. Analyst 133 (8): 984-991.

(23) Thevenot, DR., Toth, K., Durst, RA., and Wilson, GS. (2001). Electrochemical biosensors: recommended definitions and classification. Biosens Bioelectron 16 (1-2): 121-131.

(24) Jelen, F., Yosypchuk, B., Kourilov, A., Novotn, L., and Palecek, E. (2002). Label-free determination of picogram quantities of DNA by stripping voltammetry with solid copper amalgam or mercury electrodes in the presence of copper. Anal Chem 74 (18): 4788-4793.

(25) Pividori, M., Merkoci, A., and Alegret, S. (2000). Electrochemical genosensor design: immobilisation of oligonucleotides onto transducer surfaces and detection methods. Biosens Bioelectron 15 (5-6): 291-303.

(26) Brett, AMO., and Serrano, S. (1995). The electrochemical oxidation of DNA. J Braz Chem Soc 6 (1): 97-100.

(27) Singhal, P., and Kuhr, WG. (1997). Ultrasensitive voltammetric detection of underivatized oligonucleotides and DNA. Anal Chem 69 (23): 4828-4832.

(28) Kerman, K., Meric, B., Ozkan, D., Kara, P., and Ozsoz, M. Indicator based and indicator-free electrochemical DNA biosensors2001: IEEE : 3240-3243.

(29) Wang, J., Ozsoz, M., Cai, X., Rivas, G., and Shiraishi, H. (1998). Indicator-free electrochemical DNA hybridization biosensor. Anal Chim Acta 375 (3): 197-203.

(30) Kerman, K., Morita, Y., Takamura, Y., and Tamiya, E. (2003). Label-free electrochemical detection of DNA hybridization on gold electrode. Electrochem Commun 5 (10): 887-891.

(31) Eskiocak, U., Ozkan-Ariksoysal, D., Ozsoz, M., and ktem, HA. (2007). Label-free detection of telomerase activity using guanine electrochemical oxidation signal. Anal Chem 79 (22): 8807-8811.

(32) LaGier, MJ., Scholin, CA., Fell, JW., Wang, J., and Goodwin, KD. (2005). An electrochemical RNA hybridization assay for detection of the fecal indicator bacterium *Escherichia coli*. Mar Pollut Bull 50 (11): 1251-1261.

(33) Lucarelli, F., Marrazza, G., Palchetti, I., Cesaretti, S., and Mascini, M. (2002). Coupling of an indicator-free electrochemical DNA biosensor with polymerase chain reaction for the detection of DNA sequences related to the apolipoprotein E. Anal Chim Acta 469 (1): 93-99.

(34) Ozkan-Ariksoysal, D., Tezcanli, B., Kosova, B., and Ozsoz, M. (2008). Design of electrochemical biosensor systems for the detection of specific DNA sequences in PCR-amplified nucleic acids related to the catechol-O-methyltransferase Val108/158Met polymorphism based on intrinsic guanine signal. Anal Chem 80 (3): 588-596.

(35) Carter, MT., Rodriguez, M., and Bard, AJ. (1989). Voltammetric studies of the interaction of metal chelates with DNA. 2. Tris-chelated complexes of cobalt (III) and iron (II) with 1, 10-phenanthroline and 2, 2'-bipyridine. J Am Chem Soc 111 (24): 8901-8911.

(36) Erdem, A., Meric, B., Kerman, K., Dalbasti, T., and Ozsoz, M. (1999). Detection of interaction between metal complex indicator and DNA by using electrochemical biosensor. Electroanal 11 (18): 1372-1376.

(37) Yu, HZ., Luo, CY., Sankar, CG., and Sen, D. (2003). Voltammetric procedure for examining DNA-modified surfaces: quantitation, cationic binding activity, and electron-transfer kinetics. Anal Chem 75 (15): 3902-3907.

(38) Yang, IV., and Thorp, HH. (2001). Modification of indium tin oxide electrodes with repeat polynucleotides: electrochemical detection of trinucleotide repeat expansion. Anal Chem 73 (21): 5316-5322.

(39) Siddiquee, S., Yusof, NA., Salleh, AB., Tan, SG., and Bakar, FA. (2011). Electrochemical DNA biosensor for the detection of Trichoderma harzianum based on a gold electrode modified with a composite membrane made from an ionic liquid, ZnO nanoparticles and chitosan, and by using acridine orange as a redox indicator. Mikrochim acta 172 (3-4): 357-363.

(40) Kelley, SO., Barton, JK., Jackson, NM., and Hill, MG. (1997). Electrochemistry of methylene blue bound to a DNA-modified electrode. Bioconjugate Chem 8 (1): 31-37.

(41) Jin, Y., Yao, X., Liu, Q., and Li, J. (2007). Hairpin DNA probe based electrochemical biosensor using methylene blue as hybridization indicator. Biosens Bioelectron 22 (6): 1126-1130.

(42) Siddiquee, S., Yusof, N., Salleh, A., Bakar, FA., and Heng, LY. (2009). Electrochemical DNA biosensor for the detection of specific gene related to Trichoderma harzianum species. Bioelectrochemistry 79 (1): 31-36.

(43) Gu, J., Lu, X., and Ju, H. (2002). DNA sensor for recognition of native yeast DNA sequence with methylene blue as an electrochemical hybridization indicator. Electroanal 14 (13): 949-954.

(44) Wang, J., Ozsoz, M., Cai, X., Rivas, G., and Shiraishi, H. (1998). Interactions of antitumor drug daunomycin with DNA in solution and at the surface Bioelectroch Bioener 45 (1): 33-40.

(45) Marrazza, G., Chianella, I., and Mascini, M. (1999). Disposable DNA electrochemical biosensors for environmental monitoring. Anal Chim Acta 387: 297-307.

(46) Wang, S., Peng, T., and Yang, CF. (2003). Electrochemical determination of interaction parameters for DNA and mitoxantrone in an irreversible redox process. Biophys Chem 104 (1): 239-248.

(47) Latt, SA., and Stetten, G. (1976). Spectral studies on 33258 Hoechst and related bisbenzimidazole dyes useful for fluorescent detection of deoxyribonucleic acid synthesis. J Histochem Cytochem 24 (1): 24-33.

(48) Bontemps, J., Houssier, C., and Fredericq, E. (1975). Physico-chemical study of the complexes of "33258 Hoechst" with DNA and nucleohistone. Nucleic Acids Res 2 (6): 971-984.

(49) Guan, Y., Shi, R., Li, X., Zhao, M., and Li, Y. (2007). Multiple binding modes for dicationic Hoechst 33258 to DNA. J Phys Chem B 111 (25): 7336-7344.

(50) Weisblum, B., and Haenssler, E. (1974). Fluorometric properties of the bibenzimidazole derivative Hoechst 33258, a fluorescent probe specific for AT concentration in chromosomal DNA. Chromosoma 46 (3): 255-260.

(51) Embry, KJ., Searle, MS., and Crak, DJ. (1993). Interaction of Hoechst 33258 with the minor groove of the A+ T rich DNA duplex d (GGTAATTACC) 2 studied in solution by NMR spectroscopy. Eur J Biochem 211 (3): 437-447.

(52) Vega, MC., et al. (1994). Three dimensional crystal structure of the A tract DNA dodecamer d (CGCAAATTTGCG) complexed with the minor groove binding drug Hoechst 33258. Eur J Biochem 222 (3): 721-726.

(53) Sufen, W., Tuzhi, P., and Yang, CF. (2002). Electrochemical Studies for the Interaction of DNA with an Irreversible Redox Compound–Hoechst 33258. Electroanal 14 (23): 1648-1653.

(54) Choi, YS., and Park, DH. (2004). Electrochemical gene detection using multielectrode array DNA chip. Journal-KOREAN Physical Society 44: 1556-1559.

(55) Choi, YS., Lee, KS., and Park, DH. (2006). Gene detection using Hoechst 33258 on a biochip. Current Applied Physics 6 (4): 777-780.

(56) Hashimoto, K., Ito, K., and Ishimori, Y. (1994). Sequence-specific gene detection with a gold electrode modified with DNA probes and an electrochemically active dye. Anal Chem 66 (21): 3830-3833.

(57) Ahmed, MU., et al. (2007). Electrochemical DNA biosensor using a disposable electrochemical printed (DEP) chip for the detection of SNPs from unpurified PCR amplicons. Analyst 132 (5): 431-438.

(58) Ahmed, MU., Hasan, Q., Mosharraf Hossain, M., Saito, M., and Tamiya, E. (2010). Meat species identification based on the loop mediated isothermal amplification and electrochemical DNA sensor. Food Control 21 (5): 599-605.

(59) Sugaya, K., et al. (1994). Three genes in the human MHC class III region near the junction with the class II: gene for receptor of advanced glycosylation end products, PBX2 homeobox gene and a notch homolog, human counterpart of mouse mammary tumor gene int-3. Genomics 23 (2): 408-419.

(60) Hudson, B., et al. (2008). Identification, classification, and expression of RAGE gene splice variants. FASEB J 22 (5): 1572-1580.

(61) Sterenczak, K., et al. (2009). Cloning, characterisation, and comparative quantitative expression analyses of receptor for advanced glycation end products (RAGE) transcript forms. Gene 434 (1-2): 35-42.

(62) Schlueter, C., Hauke, S., Flohr, A., Rogalla, P., and Bullerdiek, J. (2003). Tissue-specific expression patterns of the RAGE receptor and its soluble forms- a result of regulated alternative splicing? BBA-Gene Struct Expr 1630 (1): 1-6.

(63) Wautier, JL., and Grossin, N. (2008). sRAGE and esRAGE. Diabetes Metab 34 (6 Pt 1): 631.

(64) Ding, Q., and Keller, JN. (2005). Splice variants of the receptor for advanced glycosylation end products (RAGE) in human brain. Neurosci Lett 373 (1): 67-72.

(65) Stephen, T. (2009). The Receptor for Advanced Glycation End Products (RAGE) and the Lung. Journal of Biomedicine and Biotechnology 2010.

(66) Schmidt, A., Du Yan, S., Yan, S., and Stern, D. (2001). The multiligand receptor RAGE as a progression factor amplifying immune and inflammatory responses. J Clin Invest 108 (7): 949-955.

(67) Thornalley, P.J. (2007). Dietary AGEs and ALEs and risk to human health by their interaction with the receptor for advanced glycation endproducts (RAGE)--an introduction. Mol Nutr Food Res 51 (9): 1107-1110.

(68) Hudson, B., et al. (2002). Glycation and diabetes: The RAGE connection. Curr Sci 83 (12): 1515-1521.

(69) Hori, O., et al. (1995). The receptor for advanced glycation end products (RAGE) is a cellular binding site for amphoterin. J Biol Chem 270 (43): 25752-25761.

(70) Hofmann, MA., et al. (1999). RAGE mediates a novel proinflammatory axis: a central cell surface receptor for S100/calgranulin polypeptides. Cell 97 (7): 889-901.

(71) Chavakis, T., et al. (2003). The Pattern Recognition Receptor (RAGE) Is a Counterreceptor for Leukocyte Integrins. J Exp Med 198 (10): 1507-1515.

(72) Deane, R., et al. (2003). RAGE mediates amyloid- peptide transport across the blood-brain barrier and accumulation in brain. Nat Med 9 (7): 907-913.

(73) Srikanth, V., et al. (2009). Advanced glycation endproducts and their receptor RAGE in Alzheimer's disease. Neurobiol Aging.

(74) Farmer, DG., and Kennedy, S. (2009). RAGE, vascular tone and vascular disease. Pharmacol Ther 124 (2): 185-194.

(75) Yan, SF., Ramasamy, R., and Schmidt, AM. (2009). Receptor for AGE (RAGE) & its Ligands – Cast into Leading Roles in Diabetes & the Inflammatory Response. J Mol Med 87 (3): 235-247.

(76) Bucciarelli, L.G., et al. (2002). RAGE is a multiligand receptor of the immunoglobulin superfamily: implications for homeostasis and chronic disease. Cell Mol Life Sci 59 (7): 1117-1128.

(77) Neeper, M., et al. (1992). Cloning and expression of a cell surface receptor for advanced glycosylation end products of proteins. J Biol Chem 267 (21): 14998-5004.

(78) Stern, DM., Yan, SD., Yan, SF., and Schmidt, AM. (2002). Receptor for advanced glycation endproducts (RAGE) and the complications of diabetes. Ageing Research Reviews 1 (1): 1-15.

(79) Goh, SY., and Cooper, ME. (2008). Clinical review: The role of advanced glycation end products in progression and complications of diabetes. J Clin Endocrinol Metab 93 (4): 1143-1152.

(80) Sakaguchi, T., et al. (2003). Central role of RAGE-dependent neointimal expansion in arterial restenosis. J Clin Invest 111 (7): 959-972.

(81) Yan, SF., Ramasamy, R., and Schmidt, AM. (2009). The receptor for advanced glycation endproducts (RAGE) and cardiovascular disease. Expert Rev Mol Med 11: e9.

(82) D'Agati, V., Yan, SF., Ramasamy, R., and Schmidt, AM. (2010). RAGE, glomerulosclerosis and proteinuria: roles in podocytes and endothelial cells. Trends Endocrinol Metab 21 (1): 50-56.

(83) Basta, G., et al. (2002). Advanced glycation end products activate endothelium through signal-transduction receptor RAGE: a mechanism for amplification of inflammatory responses. Circulation 105 (7): 816-822.

(84) Lin, L., Park, S., and Lakatta, EG. (2009). RAGE signaling in inflammation and arterial aging. Front Biosci 14: 1403-1413.

(85) Scaffidi, P., Misteli, T., and Bianchi, ME. (2002). Release of chromatin protein HMGB1 by necrotic cells triggers inflammation. Nature 418 (6894): 191-195.

(86) Orlova, VV., et al. (2007). A novel pathway of HMGB1-mediated inflammatory cell recruitment that requires Mac-1-integrin. EMBO J 26 (4): 1129-1139.

(87) Buhimschi, CS., et al. (2009). Characterization of RAGE, HMGB1, and S100β in Inflammation-Induced Preterm Birth and Fetal Tissue Injury. Am J Pathol 175 (3): 958-975.

(88) Hao, Q., Du, XQ., Fu, X., and Tian, J. (2008). Expression and clinical significance of HMGB1 and RAGE in cervical squamous cell carcinoma. Zhonghua Zhong Liu Za Zhi 30 (4): 292-295.

(89) Schenk, S., Schraml, P., Bendik, I., and Ludwig, CU. (2001). A novel polymorphism in the promoter of the RAGE gene is associated with non-small cell lung cancer. Lung Cancer 32 (1): 7-12.

(90) Sims, GP., Rowe, DC., Rietdijk, ST., Herbst, R., and Coyle, AJ. (2010). HMGB1 and RAGE in inflammation and cancer. Annu Rev Immunol 28: 367-388.

(91) Rouhiainen, A., et al. (2004). Regulation of monocyte migration by amphoterin (HMGB1). Blood 104 (4): 1174-1182.

(92) Zimmer, DB., Cornwall, EH., Landar, A., and Song, W. (1995). The S100 protein family: history, function, and expression. Brain Res Bull 37 (4): 417-429.

(93) Donato, R. (2007). RAGE: a single receptor for several ligands and different cellular responses: the case of certain S100 proteins. Curr Mol Med 7 (8): 711-724.

(94) Gerlach, R., et al. (2006). Active secretion of S100B from astrocytes during metabolic stress. Neuroscience 141 (4): 1697-1701.

(95) Ellis, EF., Willoughby, KA., Sparks, SA., and Chen, T. (2007). S100B protein is released from rat neonatal neurons, astrocytes, and microglia by in vitro trauma and anti-S100 increases trauma-induced delayed neuronal injury and negates the protective effect of exogenous S100B on neurons. J Neurochem 101 (6): 1463-1470.

(96) Moore, BW. (1965). A soluble protein characteristic of the nervous system. Biochem Biophys Res Commun 19 (6): 739-744.

(97) Leclerc, E., Fritz, G., Vetter, SW., and Heizmann, CW. (2009). Binding of S100 proteins to RAGE: an update. Biochim Biophys Acta 1793 (6): 993-1007.

(98) Cecil, D.L., et al. (2005). Inflammation-induced chondrocyte hypertrophy is driven by receptor for advanced glycation end products. J Immunol 175 (12): 8296-8302.

(99) Heizmann, CW., Fritz, G., and Schafer, BW. (2002). S100 proteins: structure, functions and pathology. Front Biosci 7: d1356-1368.

(100) Huttunen, HJ., et al. (2000). Coregulation of neurite outgrowth and cell survival by amphoterin and S100 proteins through receptor for advanced glycation end products (RAGE) activation. J Biol Chem 275 (51): 40096-40105.

(101) Vincent, AM., et al. (2007). Receptor for advanced glycation end products activation injures primary sensory neurons via oxidative stress. Endocrinology 148 (2): 548-558.

(102) Shanmugam, N., Ransohoff, RM., and Natarajan, R. (2006). Interferon-gamma-inducible protein (IP)-10 mRNA stabilized by RNA-binding proteins in monocytes treated with S100b. J Biol Chem 281 (42): 31212-31221.

(103) Fuentes, MK., et al. (2007). RAGE activation by S100P in colon cancer stimulates growth, migration, and cell signaling pathways. Dis Colon Rectum 50 (8): 1230-1240.

(104) Arumugam, T., and Logsdon, CD. (2009). S100P: a novel therapeutic target for cancer. Amino Acids.

(105) Ho, MK., and Springer, TA. (1982). Mac-1 antigen: quantitative expression in macrophage populations and tissues, and immunofluorescent localization in spleen. J Immunol 128 (5): 2281-2286.

(106) Dunne, JL., Collins, RG., Beaudet, AL., Ballantyne, CM., and Ley, K. (2003). Mac-1, but not LFA-1, uses intercellular adhesion molecule-1 to mediate slow leukocyte rolling in TNF-alpha-induced inflammation. J Immunol 171 (11): 6105-6111.

(107) Butcher, EC. (1991). Leukocyte-endothelial cell recognition: three (or more) steps to specificity and diversity. Cell 67 (6): 1033-1036.

(108) Imhof, B., Emre, Y., and Abcam. (2011). Leukocyte recruitment in inflammation.

(109) Bierhaus, A., et al. (2001). Diabetes-associated sustained activation of the transcription factor nuclear factor-kappaB. Diabetes 50 (12): 2792-2808.

(110) Thomas, T., Thomas, G., McLendon, C., Sutton, T., and Mullan, M. (1996). beta-Amyloid-mediated vasoactivity and vascular endothelial damage. Nature 380 (6570): 168-171.

(111) Selkoe, DJ. (2001). Clearing the brain's amyloid cobwebs. Neuron 32 (2): 177-180.

(112) Lue, LF., Walker, DG., Jacobson, S., and Sabbagh, M. (2009). Receptor for advanced glycation end products: its role in Alzheimer's disease and other neurological diseases. Future Neurol 4 (2): 167-177.

(113) Sakurai, S., et al., editors. Identification of a novel AGE-capturable soluble variant of the RAGE in human sera2002: Elsevier.

(114) Koyama, H., Yamamoto, H., and Nishizawa, Y. (2007). RAGE and Soluble RAGE: Potential Therapeutic Targets for Cardiovascular Diseases. Mol Med 13 (11-12): 625-635.

(115) Bopp, C., et al. (2008). sRAGE is elevated in septic patients and associated with patients outcome. J Surg Res 147 (1): 79-83.

(116) Choi, KM., et al. (2009). Association between endogenous secretory RAGE, inflammatory markers and arterial stiffness. Int J Cardiol 132 (1): 96-101.

(117) Emanuele, E., et al. (2005). Circulating levels of soluble receptor for advanced glycation end products in Alzheimer disease and vascular dementia. Arch Neurol 62 (11): 1734-1736.

(118) Geroldi, D., Falcone, C., and Emanuele, E. (2006). Soluble receptor for advanced glycation end products: from disease marker to potential therapeutic target. Curr Med Chem 13 (17): 1971-1978.

(119) Biosystem, A. Creating standard Curves with genomic DNA or plasmid DNA templates for use in quantitative PCR.

(120) Macherey-Nagel. (2010). Total RNA isolation.

(121) Horakova, P., Fojtova, M., Vytras, K., and Fojta, M. (2008). Enzyme-Linked Electrochemical Detection of PCR-Amplified Nucleotide Sequences

Using Disposable Screen-Printed Sensors. Applications in Gene Expression Monitoring. Sensors 8: 193-210.

(122) Medelon, F. Mean, Standard Deviation, and Coefficient of Variation - Westgard QC.

(123) Guan, Y., Zhou, W., Yao, X., Zhao, M., and Li, Y. (2006). Determination of nucleic acids based on the fluorescence quenching of Hoechst 33258 at pH 4.5. Anal Chim Acta 570: 21-28.

(124) Cesarone, CF., Bolognesi, C., and Santi, L. (1979). Improved microfluorometric DNA determination in biological material using 33258 Hoechst. Anal Biochem 100 (1): 188-197.

(125) Sapse, A., Mezei, M., Karakhanov, I., and Jaind, D. (1997). Solvent effect on the conformation of the Hoechst 33258 agent. J Mol Struc-Theochem 393: 25-30.

(126) Meadows, M., and Potrykus, I. (1981). Hoechst 33258 as a vital stain for plant cell protoplasts. Plant Cell Rep 1 (2): 77-79.

(127) Tanji, N., et al. (2000). Expression of advanced glycation end products and their cellular receptor RAGE in diabetic nephropathy and nondiabetic renal disease. J Am Soc Nephrol 11 (9): 1656-1666.

(128) Morcos, M., et al. (2002). Activation of tubular epithelial cells in diabetic nephropathy. Diabetes 51 (12): 3532-3544.

(129) Berrou, J., et al. (2009). Advanced glycation end products regulate extracellular matrix protein and protease expression by human glomerular mesangial cells. Int J Mol Med 23 (4): 513-520.

Biography

Miss Parinee Kittimongkolsuk. She was born on May 6, 1987 in Bangkok. In 2008, She obtained a bachelor of science degree with first class honours in Medical Technology from Allied Health Sciences faculty, Chulalongkorn University. From 2008- 2010, She did her postgraduate education in clinical biochemistry and molecular medicine at department of clinical chemistry, faculty of Allied Health of Sciences, Chulalongkorn University. She received a scholarship from Graduate School , Chulalongkorn University and received teacher assistant scholarship from faculty of Allied Health of Science, Chulalongkorn University.